

# A new middle Miocene crocidosoricine shrew from the Mongolian Shargain Gobi Desert

VLADIMIR S. ZAZHIGIN and LEONID L. VOYTA



Zazhigin, V.S. and Voyta, L.L. 2018. A new middle Miocene crocidosoricine shrew from the Mongolian Shargain Gobi Desert. *Acta Palaeontologica Polonica* 63 (1): 171–187.

The crocidosoricines are a relatively widespread subfamily of shrews with an early Oligocene to late Miocene temporal range, generally known from Europe, and, to a lesser extent, from Asia. A new discovery from the Mongolian middle Miocene locality Sharga 2 (the lower part of the Oshin Suite) adds new data to the understanding of Crocidosoricinae arising in Asia, and allows the description of a new genus and species: *Shargainosorex angustirostris* gen. et sp. nov. A large number of fossil remains (more than 200 specimens from 95–100 buried shrews) made possible the description of the morphology of the new species in detail, and even to try to reconstruct the rostrum shape and estimate the size of the skull and body. Morphologically, and apparently adaptively, the Shargain shrew was more similar to the *Sorex* species, including tooth pigmentation, but also carried a number of white-toothed shrew features (*Crocidura*, *Suncus*). Based on these findings, we can assume the spreading of *Miosorex* sensu lato from Europe to Asia during the early Miocene, when the group acquired a number of adaptive sorex-like features as a possible result of occupying new trophic niches in this part of the continent.

Key words: Mammalia, Soricidae, Crocidosoricinae, *Miosorex*, Neogene, Miocene, Shargain Gobi, Mongolia.

Vladimir S. Zazhigin [zazhvol@gmail.com], Geological Institute, Russian Academy of Sciences, Pyzhevskii per. 7, Moscow, 109017, Russia.

Leonid L. Voyta [Leonid.Voyta@zin.ru] (corresponding author), Laboratory of Theriology, Zoological Institute, Russian Academy of Sciences, Universitetskaya nab. 1, Saint Petersburg, 199034, Russia.

Received 7 June 2017, accepted 9 November 2017, available online 5 March 2018.

Copyright © 2018 V.S. Zazhigin and L.L. Voyta. This is an open-access article distributed under the terms of the Creative Commons Attribution License (for details please see <http://creativecommons.org/licenses/by/4.0/>), which permits unrestricted use, distribution, and reproduction in any medium, provided the original author and source are credited.

## Introduction

The crocidosoricines are a relatively widespread subfamily of shrews with an early Oligocene to late Miocene temporal range. They are generally known from Europe, and, to a lesser extent, from Asia, having been reported in several dozen localities (Lartet 1851; Depéret 1892; Viret and Zapfe 1951; Doben-Florin 1964; Li et al. 1983; Reumer 1987; Qiu 1988; Ziegler 1989, 1990, 2005; Rzebik-Kowalska 1993; Van den Hoek Ostende 2001, 2003; Lopatin 2004; Doukas and Van den Hoek Ostende 2006; Ziegler et al. 2007; Engesser and Storch 2008; Engesser 2009; Van Dam et al. 2011; Huguene and Maridet 2011; Huguene et al. 2012; Klietmann et al. 2013, 2014; Daxner-Höck et al. 2017). The very rich European localities comprise numerous remains that have been described as new genera and species at various times. At present, the subfamily Crocidosoricinae Reumer, 1987 incorporates the 16 genera *Taatsinia* Ziegler, Dahlmann, and Storch, 2007 (early Oligocene); *Srinitium* Huguene, 1976 (late Oligocene); *Tavoonyia* Ziegler, Dahlmann, and

Storch, 2007 (late Oligocene); *Ulmensia* Ziegler, 1989 (late Oligocene); *Crocidosorex* Lavocat, 1951 (late Oligocene, early–middle Miocene); *Oligosorex* Kretzoi, 1959 (late Oligocene, early–middle Miocene); *Carposorex* Crochet, 1975 (early Miocene); *Florinia* Ziegler, 1989 (early Miocene); *Aralosorex* Lopatin, 2004 (early Miocene); *Miocrocidosorex* Lopatin, 2004 (early Miocene); *Soricella* Doben-Florin, 1964 (early Miocene); *Clapasorex* Crochet, 1975 (early–middle Miocene); *Lartetium* Ziegler, 1989 (early–middle Miocene); *Miosorex* Kretzoi, 1959 (early–middle Miocene); and the relatively newly described *Turiasorex* Van Dam, Van den Hoek Ostende, and Reumer, 2011 (middle–late Miocene), and *Meingensorex* Huguene and Maridet, 2011 (early Miocene). The taxonomic position of the tribe Myosoricini Kretzoi, 1965, as part of subfamilies Crocidosoricinae or Crocidurinae (or the independent subfamily Myosoricinae), has been discussed by many authors for several decades (Repenning 1967; Maddalena and Bronner 1992; McKenna and Bell 1997; Reumer 1998; Quérouil et al. 2001; Hutterer 1993, 2005; Furió et al. 2007; Dubey et al. 2007), but this question still remains unresolved.

New discoveries of specimens allowed clarification of the taxonomic status and composition of some earlier described taxa. For instance, Reumer (1994) considered *Oligosorex* a junior synonym of *Crocidosorex*, but afterwards Van den Hoek Ostende (2001) reinstated its validity. During the last 10–15 years four new genera were described from Asia (Lopatin 2004; Ziegler et al. 2007), as well as new species from Asia (Lopatin 2004; Ziegler et al. 2007) and Europe (Van Dam et al. 2011; Huguenev and Maridet 2011).

The substantial remains of Asian crocidosoricines are known from a relatively small number of localities: two Mongolian Oligocene deposits, Taatsiin Gol (early Oligocene) and Tavan Ovoony Deng (late Oligocene), both of which are located in the Valley of Lakes of Central Mongolia (see Ziegler et al. 2007; Daxner-Höck et al. 2017); two Kazakhstani early Miocene (or late Oligocene following Bendukidze et al. 2009) deposits, Altynshokysu (South-Eastern Kazakhstan) and Ayaguz (Eastern Kazakhstan, see Lopatin 2004); and two early/middle Miocene Chinese deposits, Xiacaowan and Shuanggou, both of which are located in Jiangsu Province of eastern China (Li et al. 1983; Qiu 1988). Some uncertainty remains for specimens determined as “Soricidae indet.” with crocidosoricine-like features from the middle Miocene locality Tunggur (Inner Mongolia, Northern China; see Qiu 1996). Eleven forms (38 remains) from Central Mongolian deposits (early Oligocene locality: Taatsiin Gol right, Hsanda Gol, and Tatal Gol; locality Unkheltseg from Oligocene–Miocene transition) were described by Ziegler et al. (2007: 128–136) as “Crocidosoricinae gen. et sp. indet.”

Until now, members of Asian genera of the subfamily were not reported from European sites, and vice versa. Hence, there are questions about the relationships and the exchanges among European and Asian crocidosoricine groups. The Mongolian middle Miocene locality of Sharga 2, mentioned in several articles (Zazhigin and Lopatin 2000; Lopatin and Zazhigin 2003), adds new knowledge about shrew distribution within the continent and the associated morphological changes. This paper describes a new crocidosoricine shrew from Sharga 2 on the basis of more than 200 specimens of skulls, mandibles, and dentition.

*Institutional abbreviations.*—BSP, Bayerische Staatssammlung für Paläontologie und historische Geologie, München, Germany; FSL, Faculté des Sciences of Lyon, France; GIN, Geological Institute, Russian Academy of Sciences, Moscow, Russia; HLMD, Hessisches Landesmuseum Darmstadt, Germany; MNHN, National Museum of Natural History, Paris, France; SMNS, Staatliches Museum für Naturkunde, Stuttgart, Germany; ZISP, Zoological Institute, Russian Academy of Sciences, Saint Petersburg, Russia; ZMMU, Zoological Museum of the Moscow State University, Moscow, Russia.

*Other abbreviations.*—al, alveolus; ali, alveoli; AW, anterior width of tooth (measured for M1–M2); be, buccal emargination (condylar process); CIL, condylo-incisive length;

COR, height of mandibular coronoid process; csp, coronoid spicule; hc, hypocone; hfr, hypoconal flange ridge; hpt, hard palate; imc, incisivo-maxillary canal; ioc, infraorbital canal; lacd, naso-lacrimal duct; itf, internal temporal fossa; L, length of tooth; lacf, lacrimal foramen; manf, mandibular foramen; lf, lower facet (condylar process); LLF, lower condylar facet length; LML, lower molar row length; LRA, linear regression analysis; ltf, lateral temporal fossa; mbc, mandibular canal; mc, metacone; MN, Mammal Neogene zonation; MRH, mandibular ramus height; MRWc, mandibular ramus width by condylar process (distance between mandibular foramen and tip of condyle); MSL, mandibular short length (distance between paraconid of m1 and lower sigmoid notch of mandibular ramus); msst, mesostyle; mx, maxilla; nc, nasal cavity; p4(r1–2), first and second roots of p4; P4s/d, inner distance between left and right P4; pc, paracone; pcd, paraconid; PE, length of posterior emargination of upper molariform tooth (for P4–M2); PMt, position of a foramen mentale; pmx, premaxilla; ppe, perpendicular plate of ethmoid; prc, protocone; pst, parastyle; pts, pterygoid spicule; PZC, Personal Zazhigin’s Catalog of fossil specimens; R (a–b), antero-buccal root of upper molariform teeth; R (a–l), antero-lingual root of upper molariform teeth; RMA, reduced major axis; TAL, length of talonid (for m1–m2); TRW, width of trigonid (for m1–m2); uf, upper facet (condylar process); W, width of tooth (for A3, P4, M3, i1–p4, m3); Wioc, width of lateral wall of infraorbital canal; zpmx, zygomatic process of maxilla.

*Nomenclatural acts.*—The electronic edition of this article conforms to the requirements of the amended International Code of Zoological Nomenclature, and hence the new names contained herein are available under that Code from the electronic edition of this article. This published work and the nomenclatural acts it contains have been registered in ZooBank, the online registration system for the ICZN. The ZooBank LSIDs (Life Science Identifiers) can be resolved and the associated information viewed through any standard web browser by appending the LSID to the prefix “<http://zoobank.org/>”. The LSID for this publication is: urn:lsid:zoobank.org:pub:054CAB15-8246-4046-B7A3-BD6882020177. The electronic edition of this work was published in a journal with an ISSN 0567-7920, eISSN 1732-2421, and has been archived and is available from the following digital repository: APP archive: <http://www.app.pan.pl/article/item/app003962017.html>

## Geological setting

The Sharga 2 fossil locality is located about 20 km southwest of the Sharga Village in Govi-Altai Province, southwestern Mongolia, in the centre of the Shargain Gobi Desert (Depression), on the northern slope of the Ikhe-Baerkhe-Tologoi Rock. Figure 1 shows the locality of the Shargain Gobi Desert where the new crocidosoricine shrew was

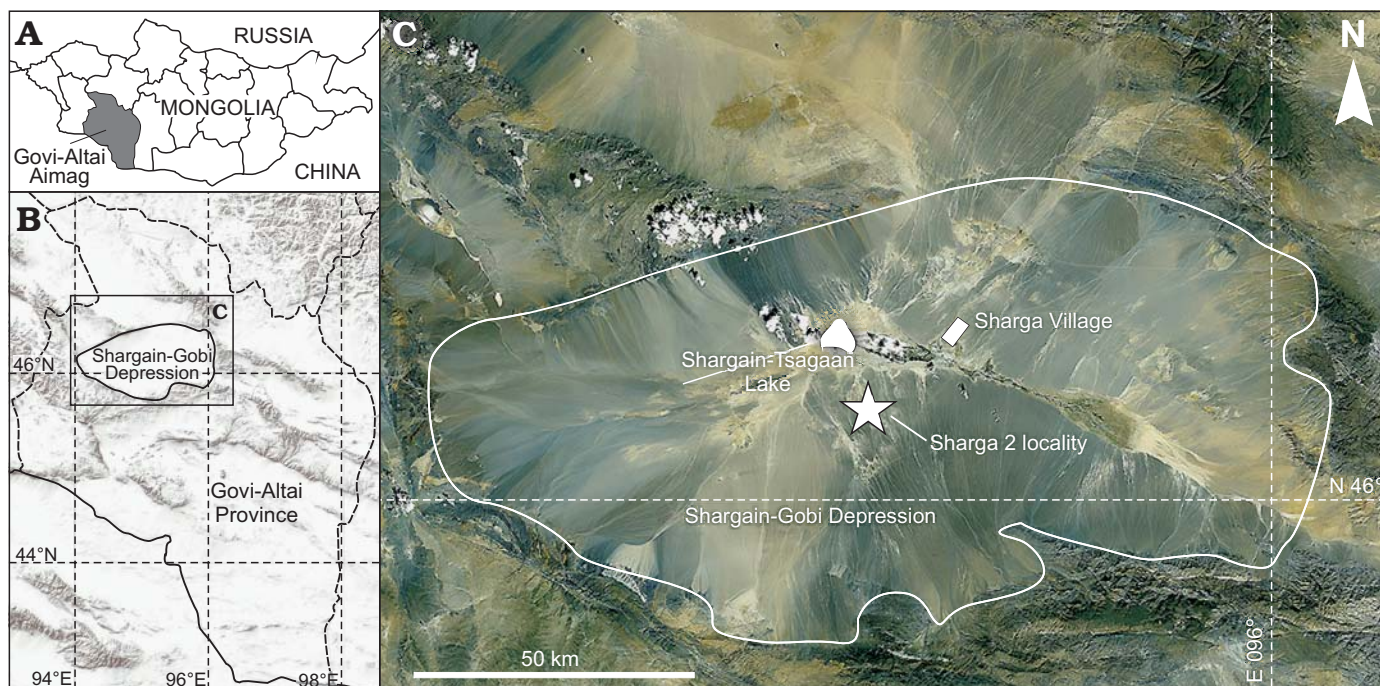


Fig. 1. Map showing location of Govi-Altai Aimag in south-western Mongolia (A) and Shargain Gobi Depression within Govi-Altai Province (B). C. Satellite image of the Sharga Village area, where *Shargainosorex angustirostris* gen. et sp. nov. was discovered.

found. The deposits consist of sand-clay lake sediments that belong to the middle Miocene Oshin Suite. Small bones of vertebrates were observed in sand-gravel lens that had a thickness of about 20 cm, and extended about 1.5 m in the lower part of profile. The large numbers of remains and rich diversity in vertebrate taxonomic groups (Pisces, Amphibia, Reptilia, Aves, and Mammalia) in the relatively small lens of littoral sediments are probably explained by continuous burying during a relatively short period (in geological sense), or sudden burial as a result of a catastrophic event (e.g., a mudflow). The remains of middle Miocene Dipodidae Fischer, 1817 and Erinaceinae Fischer, 1817 from this lens were described earlier (Zazhigin and Lopatin 2000; Lopatin and Zazhigin 2003).

## Material and methods

**Sampling.**—The material of *Shargainosorex angustirostris* gen. et sp. nov. investigated in this study comprises 218 specimens of skull and mandible fragments, as well as isolated teeth, including the type series ( $n = 23$ ), from Sharga 2, middle Miocene of Mongolia. Fossil remains were sorted into right and left fragments for estimating the minimum number of buried specimens in Sharga 2 sediments (see SOM 1: I, II, Supplementary Online Material available at [http://app.pan.pl/SOM/app63-Zazhigin\\_Voyta\\_SOM.pdf](http://app.pan.pl/SOM/app63-Zazhigin_Voyta_SOM.pdf)): 17 left fragments of skull (maxilla, premaxilla); 37/39 left fragments of mandible (dentary/semi-mandible); 7/8 left upper/lower isolated teeth; 14 right fragments of skull (maxilla, premaxilla); 53/29 right fragments of mandible (dentary/

semi-mandible); 7/5, right upper/lower isolated teeth; and two uncertain fragments. The total count of left elements ( $n = 93$ , without isolated teeth) approximately corresponds to the count of right elements ( $n = 96$ ), and the number of buried shrews probably is 95–100 specimens.

All specimens are housed in the collections of the ZISP, Russian Academy of Sciences, St. Petersburg, and listed in the “Total list of analyzed specimens” of SOM 1: I, II. Comparisons were performed using samples of *Miosorex grivensis* (Depéret, 1892) that include six specimens of skull and mandible fragments, and isolated teeth from the type locality La Grive St. Alban, middle Miocene of France. This sample is housed in ZISP, Russian Academy of Sciences, St. Petersburg (SOM 1: III). It was provided by Pierre Mein to Igor M. Gromov (and/or Alexei A. Gureev). Further comparison was based on images and measurements published in literature (details in SOM 1: IV). For estimation of different parameters (including assessment of homogeneity) and some morphological reconstruction (including skull size and rostrum shape) for *Shargainosorex angustirostris* gen. et sp. nov., we used extant shrew samples: 72 specimens of Soricinae (nine species) that are housed in ZISP and 48 specimen of Crocidurinae (18 species) that are housed in ZISP, MNHN, and ZMMU (SOM 1: V).

**Terminology.**—Dental nomenclature follows that of Reumer (1984), Dannelid (1998), and Ziegler et al. (2007). Cranial and mandibular terms follow Wible (2008). The terminology of the upper and lower unicuspid teeth of shrews is still not settled. For the purpose of this paper, we simply apply the term antemolar. Lower case letters refer to the lower dentition, and upper case letters to the upper dentition.

In the use of the term “Lipotyphla” we follow Archibald (2003), Asher (2005) and Lopatin (2006).

*Image acquisition and measurements.*—Pictures of all fragments of skulls, mandibles, and isolated teeth were obtained in needed views using digital camera (Canon EOS 60D) combined with a binocular (LOMO Micromed MSP-1) via the optical adapter (AOT-1C). The images were measured with tpsDig ver. 1.40 (Rohlf and Slice 1990) two times, to minimize the “metering error”. The analysis was performed on mean values of these replicates. The measurements mainly have been taken according to Reumer (1984), but with some changes (COR vs. MRH) and additions (Wioc, MRWc, PMt). All measurements given in mm. In the tables of SOM 7 the measurements of all studied specimens or their fragments are presented. PE-index calculated follow Reumer (1984: 6). The measurements are illustrated in SOM 2: fig. 1. High-resolution images were acquired using scanning electronic microscope (ESEM Quanta 250), with platinum sputtered surface.

*Teeth pigment analysis.*—For the record of tooth pigment, the microscope Zeiss AxioImager.A1, Zeiss Hbo 50/ac Fluorescence Mercury Light Source W, Filter Set 49 (Item Number 488049-9901-000; wavelength about 365–395 nm) was used for fluorescence histological applications, and high resolution digital camera Axio Cam MRc 5 for image acquisition. Specimens were studied in transmitted UV light. Optical images of pigmented specimens were taken using a Canon digital camera with above-mentioned additions for magnification.

*Rostrum shape reconstruction and dissection of bones.*—We tried to reconstruct the shape of the rostrum of *Shargainosorex angustirostris* gen. et sp. nov. from several fragments of the premaxilla-maxilla bones with preserved parts of the hard palate. Using drawings of rostrum fragments (for *S. angustirostris* gen. et sp. nov. and *M. grivensis*), or the whole rostrum (Recent species) on the level of the antero-buccal root of P4 and measurements of 27 Recent species of variously sized groups (see SOM 1: V), we got comparable graphic and metric material for reconstruction of muzzle and skull size. The search for metrical conformity between fossil and extant shrews was performed using LRA and RMA, which applies the minimisation of both the x and the y errors, following Miller and Kahn (1962). We have also added three measurements: CIL, MSL, and P4s/d, which allow us to compare taxa. Drawings of the rostrum for some Recent species performed through transversal dissection with the micro-drill Proxxon Miicromot 50 and the associated set of tools. Special longitudinal dissection of a mandibular fragment of *S. angustirostris* gen. et sp. nov. was obtained after placement in an epoxy resin block, with subsequent polishing.

*Statistical analysis.*—The LRA, Normality test (Shapiro-Wilk) and “Descriptive statistics” were implemented in PAST ver. 2.04 (Hammer et al. 2001). Shapiro-Wilk test was used for estimation of homogeneity of the sample from Sharga 2. This test can be correctly performed if  $3 \leq n \leq$

5000 (Shapiro and Wilk 1965; Hammer 2002; Hammer et al. 2008), although Öztuna et al. (2006) suggested that the minimum sample size was 8. Accordingly, we chose 16 measurements with  $n \geq 6$ , because the material was very fragmented; our sample contained 1–69 values (“individuals”) for different measurements.

*Illustrations.*—All the drawings were made from photographs combining Adobe Photoshop and Corel Draw. The map of Sharga 2 locality was prepared using satellite-image from resource ESRI (<http://www.esri.com/>) through Sas. Planet v.160707.9476 (tab ESRI: ArcGIS.Imagery). The images of transverse dissection of the rostrum of *Sylvisorex johnstoni* (Dobson, 1887) and *Crocidura juvenetae* Heim de Balsac, 1958 were provided by Christiane Denys (MNHN).

*Supplementary Online Material.*—SOM 1–6, contain additional information about samples, auxiliary figures, and measurements; SOM 7, measurements of each analyzed specimen.

## Systematic palaeontology

Order Lipotyphla Haeckel, 1866

Suborder Soricomorpha Gregory, 1910

Family Soricidae Fischer, 1817

Subfamily Crocidosoricinae Reumer, 1987

Genus *Shargainosorex* nov.

ZooBank LSID: <http://zoobank.org/urn:lsid:zoobank.org:act:FE820A5F-2B29-4E6D-AEC0-698DBA466A91>

*Etymology:* After the Shargain Gobi Desert (Depression), located in southwest Mongolia, the provenance of the fossil remains, and from Latin *sorex*, shrew.

*Type species:* *Shargainosorex angustirostris* sp. nov., by monotypy, see below.

*Diagnosis.*—As for the only included species.

*Stratigraphic and geographic range.*—Known only from the type locality of the species.

*Shargainosorex angustirostris* sp. nov.

Figs. 2A, C, 3A–C, E, F, 4A<sub>1</sub>, A<sub>2</sub>, 5–7, 10C; SOM 3: figs. 1A, 2; SOM 5: fig. 1.

ZooBank LSID: <http://zoobank.org/act:5CFB271C-422E-4814-8DF6-822151CF3845>

*Etymology:* From the Latin *angusti*, narrow and *rostris*, snout.

*Type material:* Holotype: ZISP 104323 (in PZC: GIN 959/1010) left dentary fragment with i1, p4–m3 (see details in SOM 1: I). Paratypes (22 fragments of premaxillary and maxillary bones, mandibles and teeth): ZISP104324/1002, 1007, 1009, 1045, 1048–50, 1055–56, 1061, 1065, 1068–69, 1071, 1073, 1080, 1097–98, 1108, 1114, 1116, 1164 (see details in SOM 1: I).

*Type locality:* Sharga 2, about 20 km SW from Sharga Village, northern slope of the Ikhe-Baerkhe-Tologoi Rock [N46°11' E 95°03'], Shargain Gobi Desert, Mongolia.

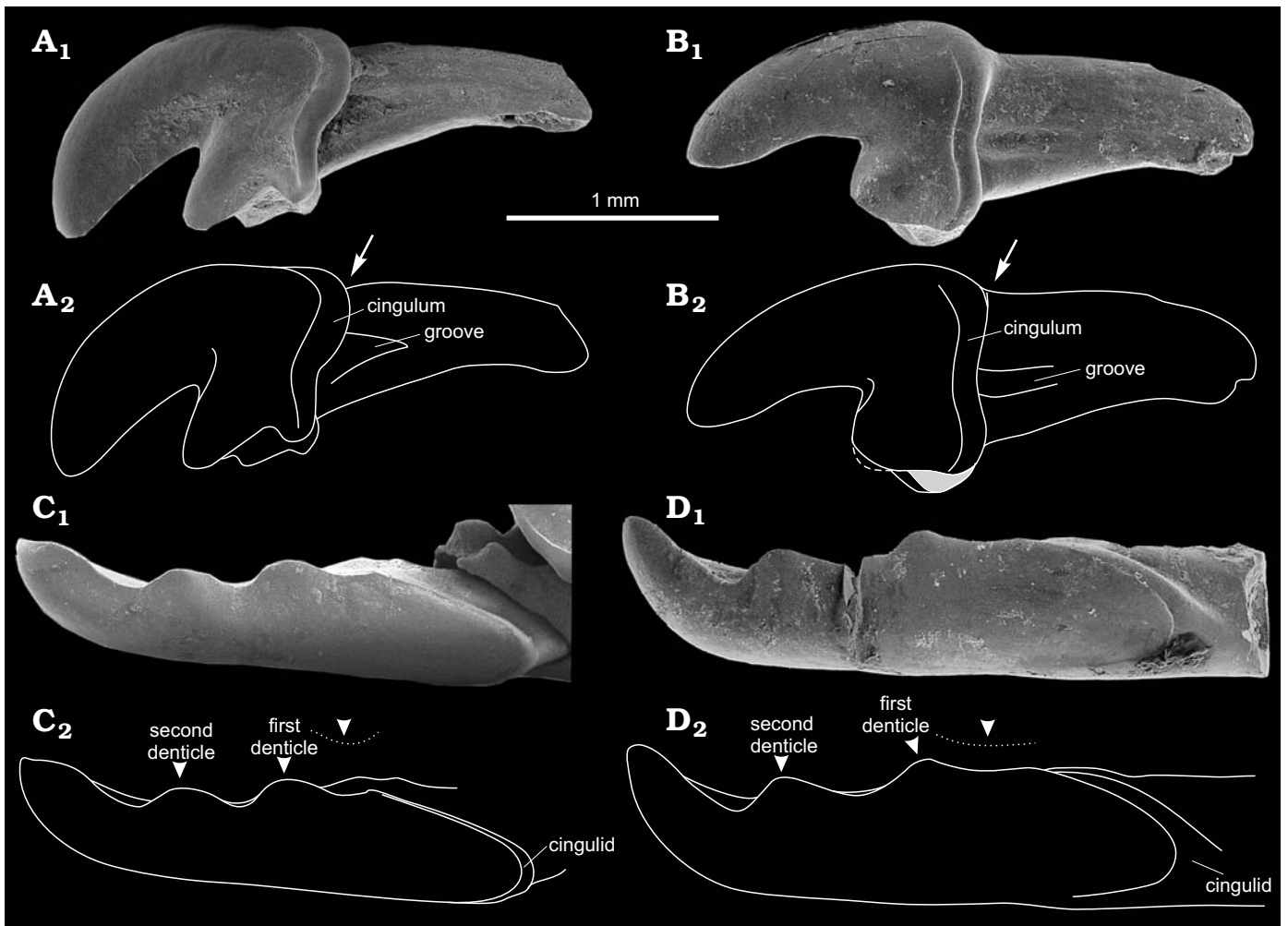


Fig. 2. Crocidosoricine shrews *Shargainosorex angustirostris* gen. et sp. nov. from middle Miocene Sharga 2 locality, Mongolia (A, C), and *Miosorex grivensis* (Deperet, 1892) from middle Miocene of La Grive St. Alban, France (B, D). A. ZISP 104324/1068 (paratype), right I1 (mirrored) in buccal view. B. ZISP 103200/6, left I1 in buccal view; dashed line and grey area on B<sub>2</sub> indicate damaged tip and base of talon. Arrows indicate crown-root junction, stepped (A<sub>2</sub>), or smooth (B<sub>2</sub>). C. ZISP 104323 (holotype), fragment of left i1 in buccal view. D. ZISP 103200/7, left i1 in buccal view. Arrowheads indicate first and second denticles of i1; dotted line indicates notch until first denticle. Photographs (A<sub>1</sub>–D<sub>1</sub>), explanatory drawings (A<sub>2</sub>–D<sub>2</sub>).

*Type horizon*.—Lower part of Oshin Suite, middle Miocene (MN7–8, ~12.5–11.2 Ma). Material was collected by VSZ during the summer of 1978, and VSZ and Evgenii V. Devjatkin (Geological Institute, Russian Academy of Sciences, Moscow, Russia) during the summer of 1979.

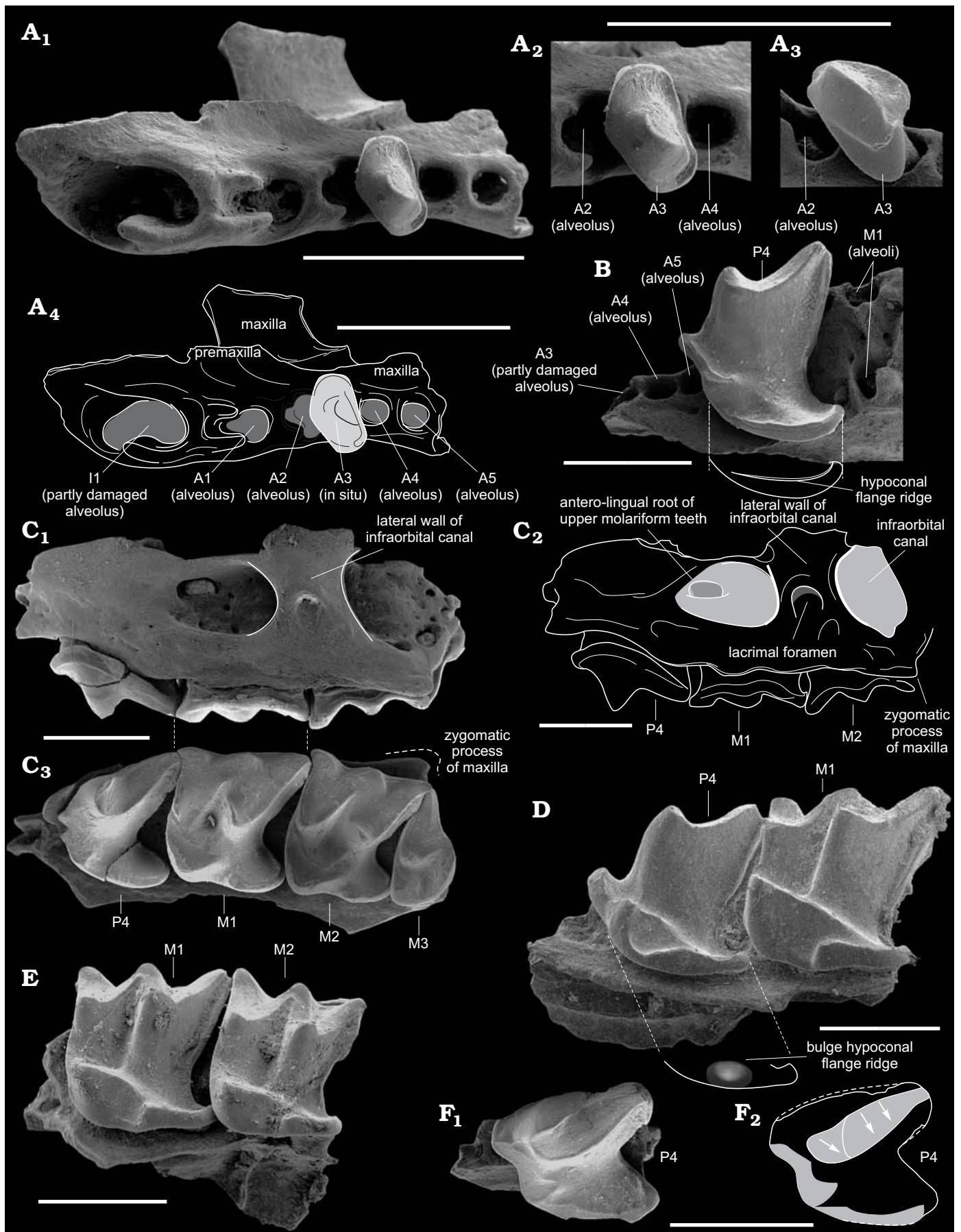
*Material*.—Type material and 195 fragments (left, right fragments of skull; left, right upper isolated teeth; left dentary, semi-mandible fragments; left lower isolated teeth; right dentary, semi-mandible fragments; right lower isolated teeth) from the type locality (see details in SOM 1: I–III).

*Measurements*.—See SOM 2 and SOM 7.

*Diagnosis*.—Small-sized shrew, with two lower antemolars (a1, p4); the first lower incisor has two denticles on the cutting edge with slightly developed notch before first denticle, its narrow ectocingulid is well developed along the posterior edge of the crown; the single root of a1 is shifted buccally relative to the longitudinal axis of the tooth crown; p4 double-rooted, with two arms of the posterocris-tid that extend posteriorly from the protoconid; ectocingulid

of lower molar well-developed; the first upper incisor has a massive crown and a rather small and wedge-shaped root; its talon is complicated, with a visible notch on its base, and a well-developed medial cusp on the talon; 5 antemolars in upper tooth row (A1–A5); the crown of the third upper antemolar is strongly compressed disto-mesially; the teeth are notably pigmented; the mental foramen lies below the protoconid of m1.

*Description*.—*Dentition*. The teeth are markedly pigmented. The dental formula is 1.5.1.3/1.1.1.3. The first upper incisor has a massive crown, and a rather small and wedge-shaped root. The apex of the incisor is not fissident. The buccal cingulum is moderately wide and well defined, and extending dorsally to the upper part of crown. The talon is complicated, with a visible notch on its base, and well-developed medial cusp of talon. The lateral side of the root has a triangle-like groove, whereas the medial side is a smooth surface. The upper outline of crown-root's junction is stepped (see Fig. 2A<sub>1</sub>, A<sub>2</sub>). Apex and talon's apex are visibly pigmented.



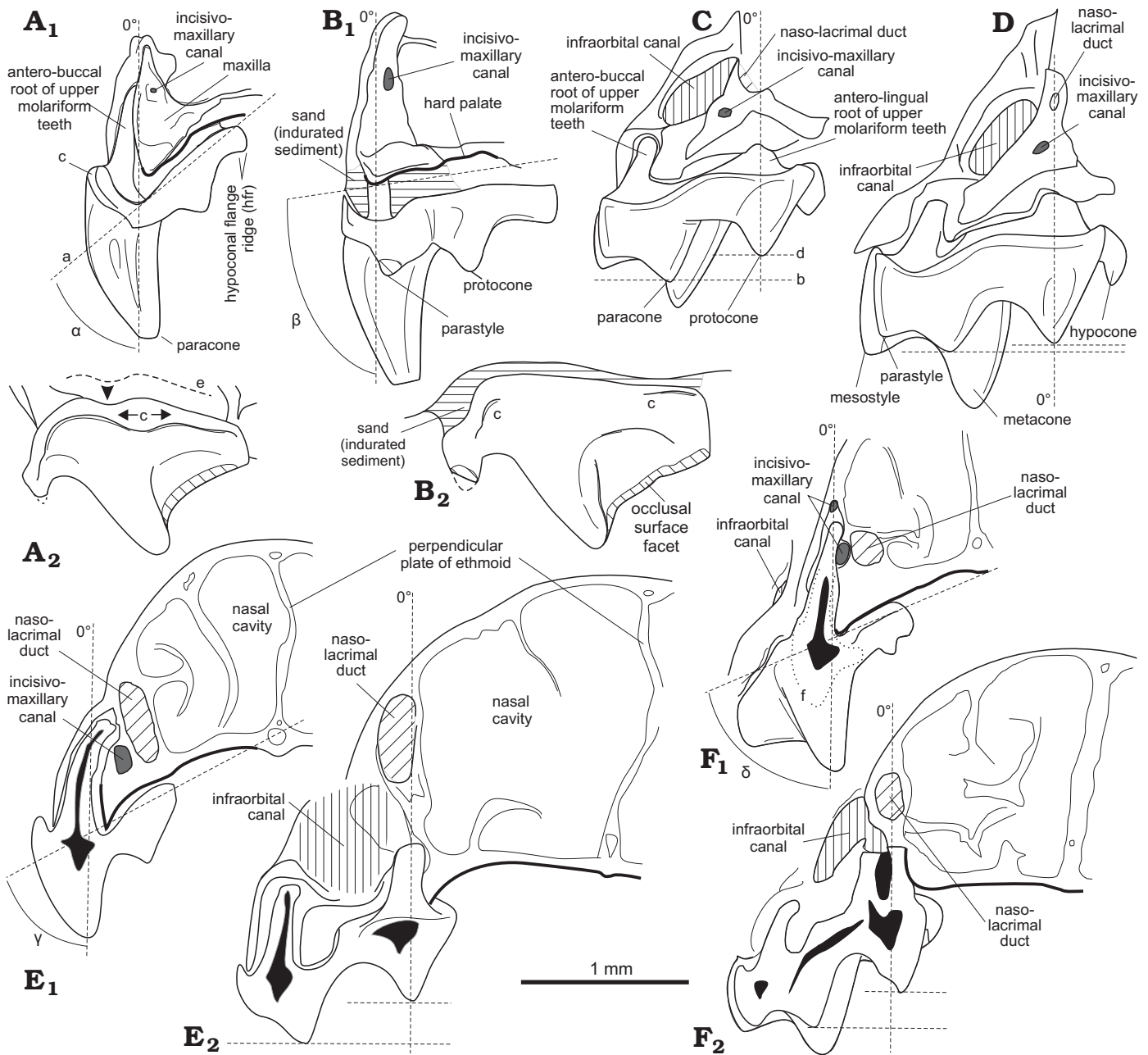


Fig. 4. Specific features of crocidosoricine shrews *Shargainosorex angustirostris* gen. et sp. nov. from middle Miocene Sharga 2 locality, Mongolia (A, B) and *Miosorex grivensis* (Deperet, 1892) from middle Miocene of La Grive St. Alban, France (C, D) compared to Recent red-toothed, *Sorex araneus* Linnaeus, 1758 (E), and white-toothed, *Suncus etruscus* (Savi, 1822) (F). A. ZISP 104324/1055 (paratype), left fourth upper premolar associated with maxilla fragment (mirrored), in anterior (A<sub>1</sub>) and buccal (A<sub>2</sub>) views. B. ZISP 103200/4, right fourth upper premolar associated with maxilla fragment, in anterior (B<sub>1</sub>) and buccal (B<sub>2</sub>) views. C. ZISP 104324/1050 (paratype), left first upper molar associated with maxilla fragment (mirrored), in anterior view. D. ZISP 103200/5, right first upper molar associated with maxilla fragment, in anterior view. E, F. Transversal sections of rostral parts of Recent shrews through P4 (level of antero-buccal root) (E<sub>1</sub>, F<sub>1</sub>), and M1 (level of anterior roots) (E<sub>2</sub>, F<sub>2</sub>). Abbreviations: a, inclination line of the hard palatine relative to antero-buccal root axis of P4; b, line of a paracone position relative to a protocone line (d) along antero-lingual root axis of M1; e, the undulated upper margin of P4 in buccal view; f, line of the ground-in surface (shown only for *S. etruscus* due to degree of its tooth preservation);  $\alpha$ – $\delta$  angles, values of the hard palatine relative inclination for each species ( $\alpha \leq 42^\circ$ ;  $\beta \approx 81^\circ$ ;  $\gamma \approx 62^\circ$ ;  $\delta \approx 66^\circ$ ).

← Fig. 3. Crocidosoricine shrews *Shargainosorex angustirostris* gen. et sp. nov. from middle Miocene Sharga 2 locality, Mongolia (A–C, E, F), and *Miosorex grivensis* (Deperet, 1892) from middle Miocene of La Grive St. Alban, France (D). A. ZISP 104324/1069 (paratype), right maxilla in occlusal view (A<sub>1</sub>, A<sub>4</sub>); A<sub>3</sub> in occlusal (A<sub>2</sub>) and buccal (A<sub>3</sub>) views. B. ZISP 104324/1045 (paratype), left maxilla in occlusal view. C. ZISP 104324/1061 (paratype), right maxilla (mirrored) with greatly worn P4–M3, in buccal (C<sub>1</sub>, C<sub>2</sub>) and occlusal (C<sub>3</sub>) views. D. ZISP 103200/4, right maxilla (mirrored) in occlusal view. E. ZISP 104324/1050 (paratype), left maxilla in occlusal view. F. ZISP 104324/1049 (paratype), left maxilla with greatly worn P4, in occlusal view (F<sub>1</sub>). Grey areas in F<sub>2</sub> indicate occlusal wear facets of P4; arrows show different directions of wear. Photographs (A<sub>1</sub>–A<sub>3</sub>, B, C<sub>1</sub>, C<sub>3</sub>, D, E, F<sub>1</sub>), explanatory drawings (A<sub>4</sub>, C<sub>2</sub>, F<sub>2</sub>). Scale bars 1 mm.

Only one fragment of the right premaxilla-maxilla with single-rooted A3 and alveoli of I1–A2, A4–A5 is present. Antemolar A3 has a single, slightly worn cusp, its crown being strongly compressed disto-mesially (Fig. 3A<sub>2</sub>) and the buccal cingulum being broad (Fig. 3A<sub>3</sub>). Alveolus of A1 is large and round in transverse section, with a developed longitudinal base for the anterior part of the root (i.e., small groove with relatively high walls); alveolus of A2 is the largest in the row, oval-shaped (i.e., compressed disto-mesially), and with a developed longitudinal base in the anterior part; the oval-shaped root could indicate a similarly compressed crown. The relative position of the alveolus of A2, and alveolus and crown of A3 indicate that A3 is likely overlapping the posterior part of the crown of A2. The alveoli of A4 and A5 are round, without additional features, the first one slightly larger than second one (probably alveolus of A4 similar in size to alveolus of A3) (see Fig. 3A<sub>1</sub>, A<sub>4</sub>). Hence, the relative size of the antemolars is likely  $A1 \leq A2 > A3 \geq A4 > A5$ .

P4 is sub-trapezoidal in shape, markedly compressed disto-mesially, with a moderately anterior shifting of the developed parastyle and protocone; the hypocone as a distinct bulb is absent, the hypoconal flange being surrounded by a narrow ridge without any bulges; posterior emargination is well developed (Fig. 3B); the upper outline in lateral view is undulate, with a visible mesial inflection (Fig. 4A<sub>2</sub>: e); buccal cingulum extends along the upper edge of tooth, sometimes with a short gap in its mesial part. In frontal view, the lingual part of P4 is strongly inclined relative to the axis of the antero-buccal root (Fig. 4A<sub>1</sub>: a); the angle of relative inclination is less than 42° (it is the minimum value compared to other studied species).

The first and second upper molars slightly decrease in size front to back, but the width of M1 is lesser than M2 (by AW mean values, see SOM 2: table 1). M1 and M2 are sub-rectangular in outline. The paracone and metacone of M1 are high and narrow; height of the paracone is about 1/2 that of the metacone; the protocone is massive and triangular in shape, with developed pre- and postprotocrista; the hypocone is absent, but there is a moderate bulge at the beginning of the hypoconal flange ridge. The styles of M1 are straight, or the parastyle is slightly hooked, e.g., for M1–M2 (see Fig. 4B<sub>2</sub>). The posterior emargination of M1 is more weakly developed than in P4, but stronger than in M2 (see values of PE-indices in SOM 2: table 1). Ectocingulum is well developed along the upper edge of M1; precingulum

is short and lies below the protocone. In frontal view, the protocone tip position is notably higher relative to the tip of the paracone (Fig. 4C: b, d).

In general, the morphology of the second molar is similar to the first with differences only seen in the relative height of the paracone (about 3/4 of the metacone's height), a weaker posterior emargination, and a more weakly developed ectocingulum (Fig. 3C<sub>2</sub>, E).

M3 is relatively short, with a slight emargination of the outline between para- and mesostyle; the paracone is the largest, its parastylar crest being notably longer than the mesostylar crest; the metacone is weakly developed; the protocone is large with a wide base.

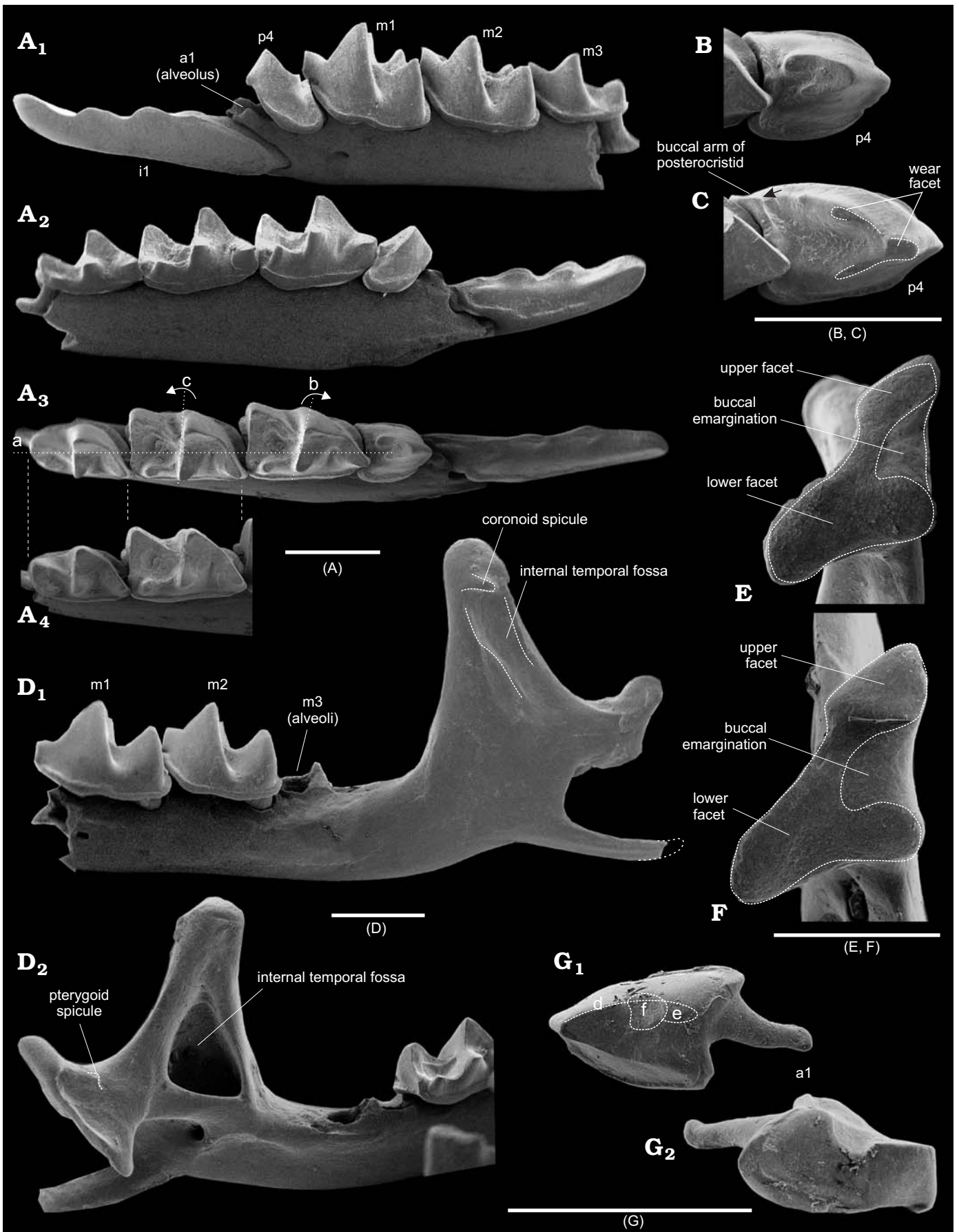
The first lower incisor is straight, with two denticles on the cutting edge (bicusplute), with a weakly developed, but defined notch before the first denticle (i.e., notch between the i1–a1 junction and first denticle); the notches of the cutting edge after the first and second denticles are equally developed; the tip of the tooth is slightly curved upwards (Figs. 2C, 5A<sub>1</sub>, A<sub>2</sub>). The ectocingulid is narrow and well developed along the posterior edge of the crown (Fig. 2C). The longitudinal axes of the incisor crown and root coincide.

The known isolated a1 is moderately worn, with the main (protoconid) cusp notably shifted anteriorly; two arms of the posterocristid extend posteriorly from the protoconid; the buccal arm (Fig. 5G<sub>1</sub>: d) extends near the medial line of the crown ends with a well-defined bulge very close to the posterior edge of the tooth (Fig. 5G<sub>1</sub>: e, G<sub>2</sub>); the degree of development of the lingual arm is not known with certainty (tooth is worn), but it presumably ends without any bulge and very close to the posterolingual part of the tooth (Fig. 5G<sub>1</sub>). The wide ectocingulid surrounds only the posterior half of the tooth (Fig. 5G<sub>2</sub>); the narrow entocingulid is well developed. The single root is shifted buccally relative to the longitudinal axis of the tooth crown (Fig. 5G<sub>1</sub>).

The p4 has an asymmetrical tetrahedral-like shape; it is double-rooted with a high protoconid and two relatively short arms of the posterocristid; the buccal arm is longer (by 1/3 of the length) than the lingual arm; the buccal arm ends in a visible cusplet, far before reaching the posterobuccal corner of tooth (Fig. 5B). The ecto- and entocingulid are wide and well developed.

The lower molars are graded in size: the first molar is the largest, the second slightly smaller, and the third even smaller (Fig. 5A). The trigonid of m1 is relatively narrow and longer than in m2 (SOM 2: table 1); with comparable length

Fig. 5. Crocidosoricine shrews *Shargainosorex angustirostris* gen. et sp. nov. from middle Miocene Sharga 2 locality, Mongolia (A, B, D, E, G), and *Miosorex grivensis* (Deperet, 1892) from middle Miocene of La Grive St. Alban, France (C, F). **A.** ZISP 104323 (holotype), left dentary fragment, in buccal (A<sub>1</sub>), lingual (A<sub>2</sub>), and occlusal (A<sub>3</sub>, A<sub>4</sub>) views. **B.** ZISP 104323 (holotype), left fourth lower premolar in occlusal view. **C.** ZISP 103200/1, left fourth lower premolar in occlusal view, showing buccal arm of posterocristid extending before entocingulid of p4 (contact indicated by arrow). **D.** ZISP 104324/1114 (paratype), fragment of the left semi-mandible, whole mandibular ramus with slightly damaged angular process, in lateral (D<sub>1</sub>) and medial (D<sub>2</sub>) views. **E.** ZISP 104324/1108 (paratype), right condyle in articular surface view. **F.** ZISP 103200/2, left condyle (mirrored) in articular surface view. **G.** ZISP 104324/1097 (paratype), right first lower antemolar in occlusal (G<sub>1</sub>) and buccal (G<sub>2</sub>) views. Abbreviations: a, line indicating the longitudinal axis of tooth crown; b, dotted line with right-turned arrow indicates notable anterior tilting of protocristid of m1 relative line a; c, dotted line with left-turned arrow indicates weak tilting of protocristid of m2; d, buccal arm of the posterocristid; e, cusplet that ends buccal arm of the posterocristid; f, deep wear facet of a1. Scale bars 1 mm.



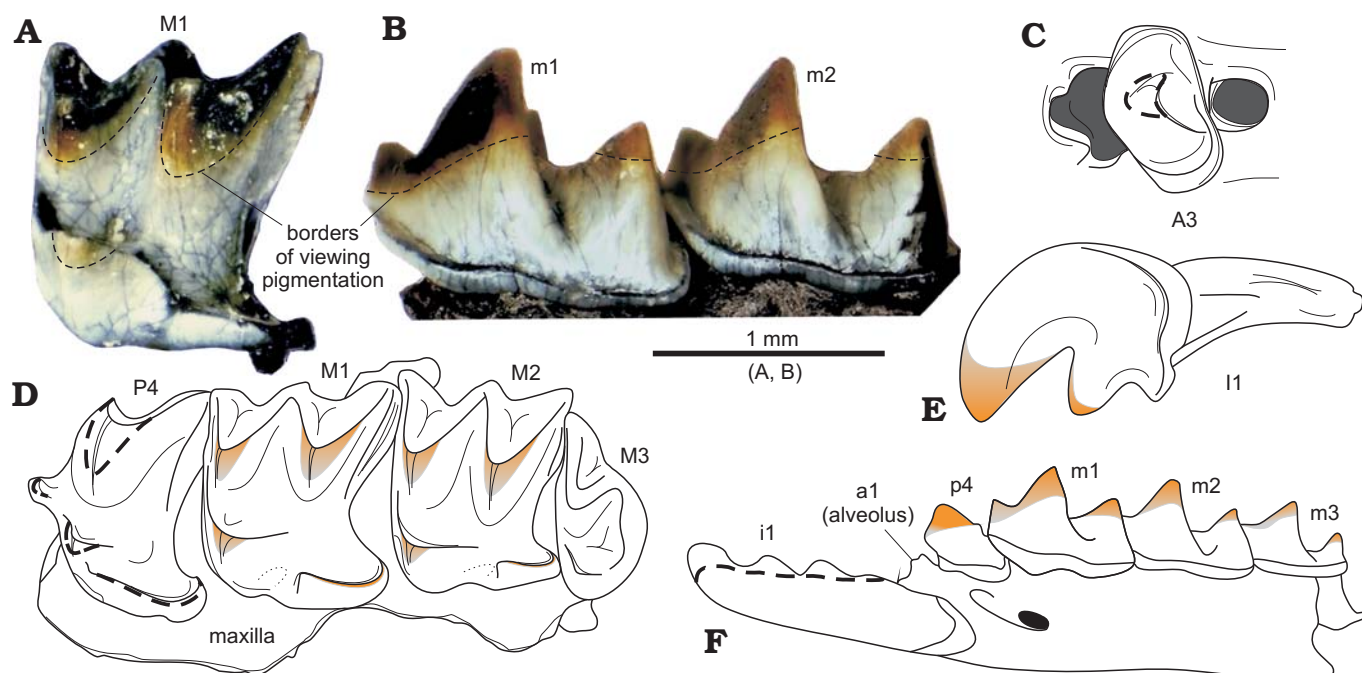


Fig. 6. Tooth pigmentation of crocidosoricine shrew *Shargainosorex angustirostris* gen. et sp. nov. from middle Miocene Sharga 2 locality, Mongolia. **A.** ZISP 104324/1080 (paratype), right M1 (mirrored), with pigmentation of main cusps, in occlusal view. **B.** ZISP 104325/1121, right dentary fragment (mirrored) in buccal view. **C.** ZISP 104324/1069 (paratype), right A3 in occlusal view. **D.** ZISP 104324/1055 (paratype), left maxilla in occlusal view. **E.** ZISP 104324/1068 (paratype), right I1 (mirrored) in buccal view. **F.** ZISP 104323 (holotype), left dentary fragment in buccal view. Dashed lines (C, D, F) indicate supposed pigment parts. Optical photographs (A, B), diagrammatic reconstructions of teeth coloration (C–F). C–F not to scale.

of talonids (mean = 0.46 mm) of both molars, the trigonid of m1 is 60.4% of the total length of the tooth, and the trigonid of m2 = 56.9%. The paraconid of m1 extends anteriorly; the protoconid is high; the metaconid is developed and slightly shifted relative to the lingual outline of the tooth base; the hypoconid is lower (by 1/2 of its height) than the protoconid; the entoconid is well developed, the entocristid reaches the base of the metaconid; the well-defined hypolophid ends in a narrow hypoconulid; the hypoconulid is widely separated from the entoconid, and slightly inclined backward; the posterobuccal ridge is weakly developed and ends far before reaching the ectocingulid; the buccal re-entrant valley is well defined; the protocristid is moderately inclined relative to the longitudinal axis of the crown (Fig. 5A<sub>3</sub>: b). The pre-, ecto-, postero-, and entocingulid are well developed.

The lower second molar repeats the morphology of m1, the differences being a relatively shorter trigonid and a generally shorter tooth; the protocristid is longer than in m1 and is almost perpendicular to the longitudinal axis of the crown (Fig. 5A<sub>3</sub>: c).

The lower third molar has a developed trigonid, and a talonid reduced in size; the talonid is narrow, with a shallow basin; the entoconid is weakly developed; the entocristid is short and does not reach the base of the metaconid; the hypoconulid is not developed; the posterobuccal ridge is weakly developed, but almost reaches the ectocingulid; the protocristid is perpendicular to the longitudinal axis of crown (similar to m2); the postcingulid is weakly developed (Fig. 5A).

**Tooth pigmentation:** Because of taphonomic conditions, not all investigated teeth display pigmentation. Many teeth

with worn tips (unpigmented) were subjected to chemical infiltration and formed a dark, unicolour secondary pigment. Some upper and lower teeth demonstrate a visible reddish soricine-like pigment on the main cusps (SOM 3: fig. 2) teeth. In addition, to detect lost pigmentation, we investigated several teeth under transmitted UV lights; this revealed that pigmented areas were notably smaller than in *Sorex daphaenodon* Thomas, 1907 (SOM 3: fig. 1). Examination of all visibly pigmented and UV analysed teeth allowed us to reconstruct the tooth colouration of *S. angustirostris* gen. et sp. nov. (Fig. 6).

**Skull fragments:** Only a few fragments of maxilla with small parts of palatal bone, and one fragment of maxilla with a small part of premaxilla, were present in the studied material. *S. angustirostris* gen. et sp. nov. has a moderately wide lateral wall of the infraorbital canal, similar in relative size to crocidurine species. Its lacrimal foramen is at the height of the M1–M2 joint, and lies centred in the lateral wall of the infraorbital canal. The end of the antero-lingual root of M1 goes into the infraorbital canal with a relatively large foramen (Fig. 3C<sub>1</sub>, C<sub>3</sub>). The relatively small zygomatic process of the maxilla extends weakly laterally; its tip is at the level of M2 metastyle (Fig. 3C<sub>2</sub>). A fragment of rostrum with alveoli of I1–A2, A4–A5, and A3 in situ shows in frontal view a “pectiniform” base of the antemolar row (not shown in figures), i.e., probably a narrow and strongly concave hard palate along the row.

**Mandible:** The horizontal ramus of the lower jaw is narrow and moderately gracile; its lower margin runs in a very shallow convex inward curve. The mental foramen lies in a

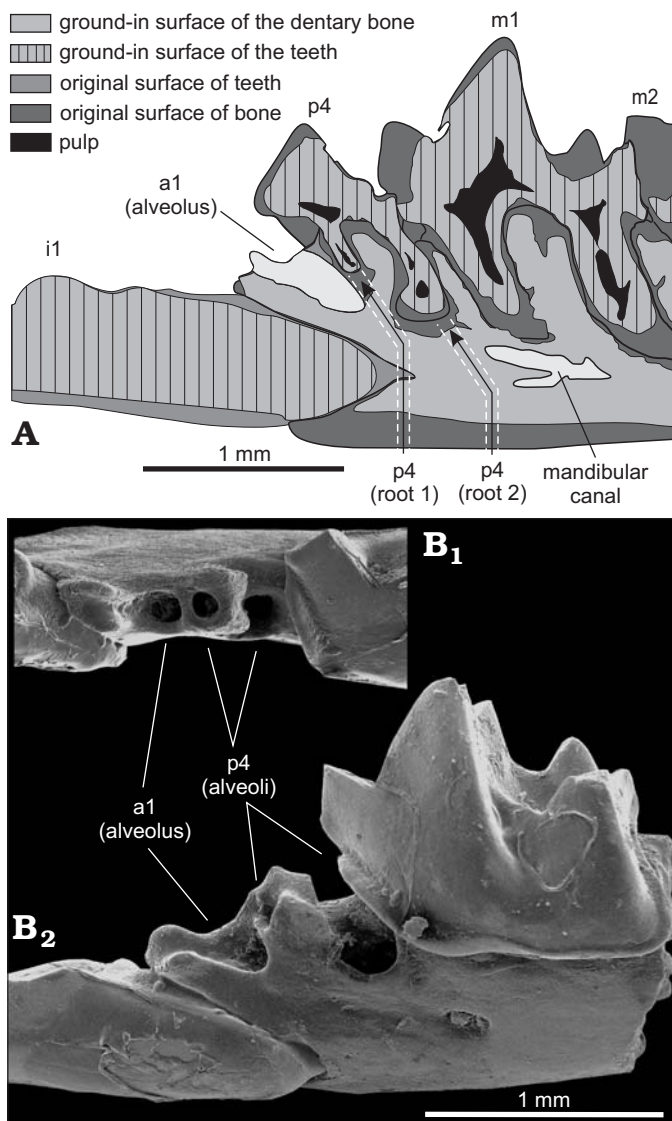


Fig. 7. Number and relative position of the lower antemolar alveoli of crocidosoricine shrew *Shargainosorex angustirostris* gen. et sp. nov. from middle Miocene Sharga 2 locality, Mongolia. **A.** ZISP 104324/1098 (paratype), longitudinal (parasagittal) section of the left dentary fragment in buccal view. **B.** ZISP 104324/1002 (paratype), right dentary fragment (mirrored) in occlusal (**B<sub>1</sub>**) and buccal (**B<sub>2</sub>**) views.

slightly tilted groove under the protoconid of m1 (Fig. 5A<sub>1</sub>). The mandibular ramus is moderately high; the coronoid process is slightly inclined anteriorly; the coronoid spicule is short and well developed; the lateral temporal fossa is shallow and notably limited by longitudinal ridges (Fig. 5D<sub>1</sub>); the internal temporal fossa is deep and clearly delineated (Fig. 5D<sub>2</sub>). The condylar process is moderately massive; the pterygoid spicule is weakly developed and lies below the margin of the upper sigmoid notch; its articular surface is sub-triangular, with a narrow contact between the upper and lower facets, and developed buccal emargination (Fig. 5E), i.e., it is crocidurine-like. The angular process is long and narrow, without developed ridges; its tip is unknown.

We investigated the number of lower antemolar alveoli and p4 roots because some dentary fragments with lost

antemolars display three alveoli: the middle alveolus is the smallest, and perhaps corresponds to vestigial a2. A longitudinal section of the left dentary fragment (Fig. 7A) reveals two differently sized roots of p4, and an anterior alveolus of a1. Three alveoli (Fig. 7B) between i1 and m1 of *S. angustirostris* gen. et sp. nov. correspond to a single-rooted procumbent a1 and a double-rooted p4.

**Variation.—Sharga 2 sample homogeneity:** To determine whether the studied fossil remains belong to a single population, i.e., whether we deal with one species, we applied statistical analyses that included an estimate of sample homogeneity in comparison to samples from local populations of *Crociodura shantungensis* Miller, 1901 and *Sorex minutus* Linnaeus, 1766 (see details in SOM 1: V), which were collected during several months of a single year. Interspecies comparisons of the test values allowed us to assess whether fossil remains were buried for a relatively short time in a restricted area. A normality test (SOM 2: tables 1–3) shows homogeneity in most metrics of the studied remains of *Shargainosorex angustirostris* gen. et sp. nov. from Sharga 2 ( $W = 0.928–0.991$ ,  $p > 0.05$ ). A visual examination of the simple graphs (specimens/values) revealed rather narrow limits of their variation, which were comparable with representative samples of *C. shantungensis* and *S. minutus* (SOM 2: table 4). The next step of the assessment of homogeneity was estimation of variability limits using coefficient of variation (CV%). Analysis of 36 measurements ( $n > 5$ ) showed comparable CV values between fossil material and the two Recent samples (SOM 2: table 5).

**Metric variations:** Normality tests and coefficient variation obtained for *Shargainosorex angustirostris* gen. et sp. nov. show several characters with wide variability limits, such as MRWc ( $W = 0.846$ ,  $p < 0.05$ ), LLF ( $W = 0.876$ ,  $p < 0.05$ ), according to a Shapiro-Wilk test (SOM 2: table 1), and features of lower (TAL[m1], TRW[m1]) and upper (PE[P4]) teeth, according to the values of their coefficient variations (SOM 2: table 5).

**Age variations:** The sample contains teeth with different degrees of age-related wear. Some teeth demonstrated heavily worn occlusal surfaces, which we can describe for one specimen (Fig. 3C<sub>2</sub>). P4 has two wide wear facets on the postparacrista; one prolonged wide facet from the parastyle to the protocone; and a narrow facet along the ridge of the hypoconal flange (Fig. 3C<sub>2</sub>, F). M1 has a mostly worn paracone and protocone; the tip of metacone is less worn than the premetacrista; the hypoconal ridge is slightly worn. In general, the tooth displays two wear facets: a broad buccal one, and a weaker protoconal one. M2 has similar wear conditions to M1, but weaker wear of the paracone and more heavy wear of the postprotocrist (Fig. 3C<sub>2</sub>). These observations further allow us to use mesowear methods (Koenigswald 2016; Hooker 2017) to compare *S. angustirostris* gen. et sp. nov. with other extinct (*Miosorex*) and Recent genera (unpublished material).

**Qualitative features:** Most variability was found in tooth pigmentation and the shape of the condylar articulation

surface. Pigmentation depends on taphonomic conditions and the chemical composition of the deposits, as mentioned above. As a result, we observe pigmented teeth (from weak orange to notably reddish colouration), unpigmented teeth (uncoloured patterns throughout the crown from grey to cream to black), and spotted teeth (areas filled with different shades of grey, brown, and black). Condylar surfaces reveal several morphotypes (SOM 5: fig. 1) with lower facets tilted relative to upper facets, and upper facets varying in width. In general, we observe typical morphotypes (Fig. 5E, SOM 5: fig. 1A, D, E), and some deviating morphotypes (SOM 5: fig. 1B, C, F). Other features do not vary notably. Namely, the mental foramen is sometimes slightly shifted anteriorly, not reaching paraconid level of m1; the protocristid of m2 demonstrates a fairly large tilting of the protocristid, like in m1 (Fig. 5A<sub>3</sub>: b), and, as a result, some isolated lower molars were misidentified. The mandibular foramen is slightly shifted anteriorly in part of the specimens.

**Comparisons.**—*Shargainosorex* gen. nov. differs from *Srinidium* (a1–a5, p4), *Taatsinia* (a1–a4, p4), *Tavoonyia*, *Ulmensia*, *Crocidosorex*, *Oligosorex*, *Carposorex*, *Clapasorex*, *Lartetium* (a1–a3, p4), *Florinia*, *Miocrocidosorex*, *Soricella*, *Meingensorex*, *Miosorex* (a1, a2, p4) in the number of lower antemolars: a1, p4. Although the number of lower antemolars is not known for the genera *Aralosorex* and *Turiasorex*, *Shargainosorex* gen. nov. differs from *Aralosorex* in the relative length of the posterocristid arms of p4 (Lopatin 2004: 212, see diagnosis); namely, the new genus is demonstrated as having a longer (by 1/2 of the length) buccal arm than the lingual arm, and the buccal arm not connecting with the ectocingulid; and in the absence of a connection between the posterobuccal crest of protoconid and ectocingulid of m1–m3 (*Aralosorex* conditions see Lopatin 2004: 213–215, fig. 2a). Moreover, *Shargainosorex* gen. nov. differs from *Turiasorex* in proportions and specific features of the teeth, e.g., absence of the middle and posterior parts of the ectocingulid of lower molars, and the transverse elongation of the upper molars (Van Dam et al. 2001: 301, fig. 1). It differs from the genera of Crocidurinae in having pigmented teeth and five upper antemolars. It differs from the genera of Soricinae in several crocidurine-like features, such as the shape of the mandibular condyle, the shape of the mandibular symphysis, the width of the lateral wall of infraorbital canal, and the composition of the mental foramen (situated in the inclined groove).

*Shargainosorex angustirostris* gen. et sp. nov. differs from *M. grivensis* (in addition to the main differential character) in the general proportions of I1. Specifically, *M. grivensis* displays a smooth dorsal outline, shorter buccal cingulum, comparable size of crown and root, and an elongated shape of the lateral groove of its root (see conditions in Fig. 2B). *M. grivensis* displays a bulged ridge in the hypoconal flange of P4 (Fig. 3D), a relatively straight upper outline and intermittent buccal cingulum, a comparably obtuse angle between the lingual part of P4 and its root (*S. angustirostris* gen. et sp. nov., angle  $\alpha \leq 42^\circ$  vs *M. griven-*

*sis*, angle  $\beta \approx 81^\circ$ ), the relative positions of the parastyle to the protocone of P4, and the paracone to the protocone of M1 (*S. angustirostris* gen. et sp. nov. has a higher position of both protocones; cf. Figs. 4A, C and 4B, D); in several features of the lower incisor, where *M. grivensis* displays a more hooked tip of i1 (a deeper distal notch after the second denticle), and the ectocingulid expanding downwards (Fig. 2D); in features of the occlusal surface of p4: *M. grivensis* has longer arms of the posterocristid that form a wide and clearly delineated basin, and the buccal arm reaches the postero-buccal margin of the tooth (Fig. 5C, “arm”).

*Shargainosorex angustirostris* gen. et sp. nov. differs from *Miosorex desnoyersianus* (Lartet, 1851) and is similar to the *M. grivensis* conditions of the occlusal shape of p4 and the more posterior position of the mental foramen. On the other hand, *M. desnoyersianus* displays a condition of the cutting margin of i1 and a development of its ectocingulid similar to the Shargain shrew (see Engesser 2009: 17, figs. 6b, f).

**Stratigraphic and geographic range.**—At present, restricted to the type locality and horizon.

## Discussion

**General remarks.**—According to Reumer (1987, 1994) the subfamily Crocidosoricinae is characterised by a diagnosis that includes a notable feature of p4, namely “... its wear surface is V-shaped”. Based on this characteristic of p4, and some other features of the lower incisor (the outline of the cutting edge) and molars (the development of cingulid and talonid on m3), we previously identified material from Sharga 2 as belonging to *M. grivensis*. The discovery of Pierre Mein’s material from La Grive in the ZISP, allowed the identification of marked differences in general size between Mongolian material from Sharga 2 and the material of *M. grivensis* from the type locality. More detailed analysis indicates the following: (i) Both the Sharga 2 and La Grive specimens have a V-shaped wear surface on p4, but display differences for several minor features. (ii) Material from Sharga 2 undoubtedly has two lower antemolars and three alveoli between i1 and m1 (see Fig. 7) and *M. grivensis* certainly has three antemolars and four alveoli (Huguency et al. 2012: 36, fig. 6A). Therefore, subsequent comparisons included two additional species: *Miosorex pusilliformis* (Doben-Florin, 1964) and *M. desnoyersianus*, which bear two/three lower antemolars. (iii) Detailed study of published materials and pictures of *M. pusilliformis* and *M. desnoyersianus* (SOM 1: IV) revealed that both species clearly differ in the number of lower antemolar alveoli (three and four alveoli, respectively), contrary to Klietmann’s et al. (2013) opinion about “taphonomic reasons in process of lacking of vestigial antemolars”, and the invalidity of *M. pusilliformis*. Type material from Wintershof-West (Doben-Florin 1964) and from Sansan (Engesser 2009), and additional material from German sites Erkertshofen 2, Petersbuch 2,

and Stubersheim 3 (Ziegler 1989) confirm the species-level status of *M. pusilliformis*. This opinion certainly requires further detailed study, but we paid attention on Klietmann's et al. (2013) interpretation of the number of lower antemolar alveoli. Figure 8 indicates the numbers of lower alveoli between i1 and m1 of *M. pusilliformis* from type localities (Fig. 8A), Stubersheim 3 (Fig. 8B), and *M. desnoyersianus* from Sansan (Fig. 8C). The position of the alveoli of *M. pusilliformis*, their number, and size correspond to similar conditions of *Shargainosorex angustirostris* gen. et sp. nov. (see Fig. 7). (iv) The number of lower antemolars became the basis for defining relations among taxa of *Miosorex* s. lato, and allowed us to distinguish a new genus with one species, *Shargainosorex angustirostris* gen. et sp. nov. Further analysis of original material from type localities of the species of the genus *Miosorex* will make it possible to consider the taxonomic position and validity of *M. pusilliformis* (Doben-Florin, 1964).

**Remarks on variability.**—Tooth pigmentation is an important character for species diagnoses and reveals evolutionary directions in the morphological development/changes of the studied species. Tooth pigment was detected using the naked eye or UV light. However, UV light is very rarely mentioned in the materials and methods sections of articles where information about teeth colouration is provided. Unicoloured fossil teeth could be underestimated, similar to the “white” teeth of Recent Asian members of the genera *Anourosorex* Milne-Edwards, 1872, *Chimarrogale* Anderson, 1877, and *Nectogale* Milne-Edwards, 1870 (Repenning 1967: 5; Danellid 1998: 169). In addition, some authors have discussed several cases of pigment variation (pigment is present/pigment is weak/unicolour) within a single-species sample; for example, Rofes et al. (2012) mentioned a possible disappearance of pigment under the influence of taphonomic conditions in the type specimen of *Nesiotites ponsi*. Later, Furió and Pons-Monjo (2013: 4, fig. 2.1, 2.2) discussed very weakly pigmented teeth or “differential pigmentation” within similar material. Mass fossil material allows the assessment of differential pigmentation, which is most likely connected with taphonomy and the chemical composition of the deposits. Observations of different colourations of fossil teeth from Sharga 2 (including UV investigation) addresses this problem. Doben-Florin's (1964) and Ziegler's (1989) descriptions of mass material of *M. pusilliformis* and *M. desnoyersianus* do not confirm differential pigmentation of these species. In addition, Klietmann's et al. (2013) study of chemical elements of fossil shrew teeth from Petersbuch 28, using an energy dispersive X-ray spectrometry (EDS) system, did not investigate iron in the lower antemolars of *M. desnoyersianus* (Klietmann et al. 2013: supplementary material), though tooth pigment can be detected with the EDS-method, e.g., fossil teeth of *Multituberculata* (Smith and Codrea 2015), and Recent teeth of shrews (Strait and Smith 2006; Dumont et al. 2014). Therefore, “points of teeth pigmented” from Engesser's (2009) emended diagnosis of

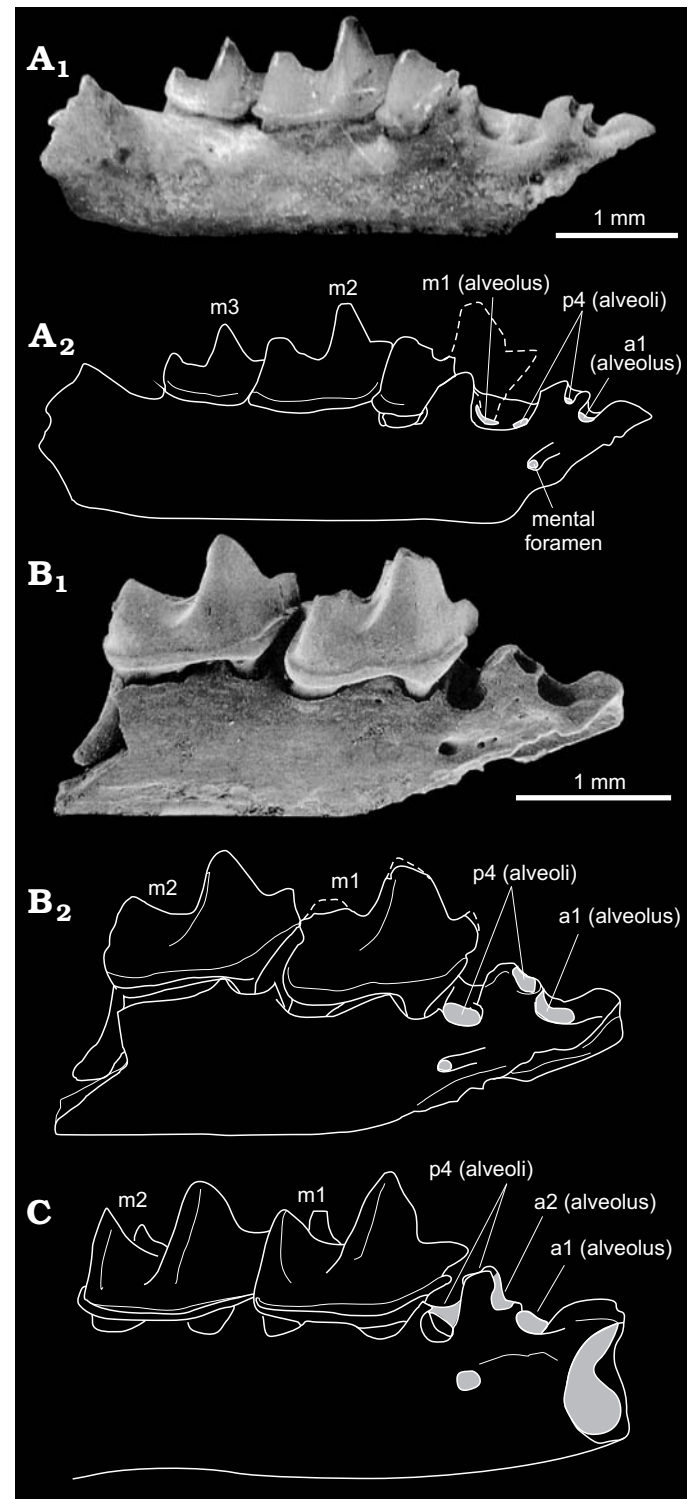


Fig. 8. Comparison of the alveoli of crocidosoricine shrews *Miosorex pusilliformis* (Doben-Florin, 1964) (A, B), and *Miosorex desnoyersianus* (Lartet, 1851) (C). A. BSP 10607 (paratype) from Wintershof-West, Germany, MN3, early Miocene; right dentary fragment (from Doben-Florin 1964: 89, pl. 3: 1a). B. SMNS#44716\_B3 from Stubersheim 3, Germany, MN3–4, early Miocene; right dentary fragment (from Ziegler 1989: 67, pl. 3: 7b). C. FSL 66225 from Sansan, France, MN6, middle Miocene; right dentary fragment (from Engesser 2009: 21, fig. 11C). Dashed line, reconstructed anterior half of m1; grey areas, alveoli and foramina opening. Optical photograph (A<sub>1</sub>), SEM photograph (B<sub>1</sub>), explanatory drawings (A<sub>2</sub>, B<sub>2</sub>, C).

*M. desnoyersianus* requires clarification. Also teeth pigmentation of *M. grivensis* from La Grive L7 by Hugueney et al. (2012) requires clarification.

The variability of the condylar surface shape of the Shargain shrew (SOM 5: fig. 1) is comparable to that described for modern shrew species. Our study of Ethiopian crocidurine species (Lavrenchenko et al. 2016) demonstrated the uselessness of condylar shape for diagnoses of similar-sized species; morphotypes of condylar shape vary widely (SOM 5: fig. 2). Sketches of the posterior surface of the condylar process of *Crocidura*, a Mediterranean taxon from Sarà et al. (1990), also display variability. Zaitsev and Rzebik-Kowalska (2003) distinguished two morphotypes of condylar surface from 25 species of *Sorex*. Hence, condylar surface shape cannot be used for the inter-species diagnostics, but is suitable for characterizing groups of species because it preserves large-scale features such as the degree of development of the contact of upper and lower facets, and buccal emargination. According to the wide variability of this feature, studies of additional material of European species of *Miosorex* are required.

**Rostrum shape reconstruction and skull size.**—*Shargainosorex angustirostris* gen. et sp. nov. displays some specific features that indicate small size of body and skull, but relatively large teeth and a narrow muzzle. Comparison of the average values of several mandibular measurements of five species reveals the smaller size of the Shargain shrew in mandibular ramus height, but similar tooth dimensions LML and L(m1) with *C. shantungensis* (SOM 6: fig. 1); *M. grivensis* is significantly larger, and *M. pusilliformis*/*M. desnoyersianus* slightly smaller. Calculation of the “large teeth index”, where the length of m1 is divided by the mandibular ramus height (MRH), for the same five species reveals that *M. pusilliformis*/*M. desnoyersianus* has the largest m1 (L is 39.6% of MRH), *S. angustirostris* gen. et sp. nov. is slightly smaller (37.8%), *S. minutus* has an intermediate value (38.04%), and *M. grivensis* and *C. shantungensis* are the smallest (36.2% and 33.4%, respectively). Thus, the relative tooth size of *S. angustirostris* gen. et sp. nov. is similar to *Sorex* (at least among small-sized species). If we assume a *sorex*-like lifestyle, then we can compare the Shargain shrew with *S. caecutiens*, because these species have the sharpest corner of the lingual part of P4 and probably similar skull and body sizes (see below). Hence, a lifestyle similar to *S. caecutiens*, with small- and middle-sized coleopterans as an important diet item (Zaitsev et al. 2014), could be hypothesized for *S. angustirostris* gen. et sp. nov. Apart from beetles and grubs, it may have consumed mollusks and plant seeds. This hypothesis should be checked by means of enamel microwear investigations.

The available premaxilla-maxilla fragments (Figs. 3A<sub>1</sub>, 4A<sub>1</sub>) showed an unusual tilting of the lingual part of P4; it is strongly inclined relative to the axis of the antero-buccal root (Fig. 4A<sub>1</sub>: a) and the angle of relative inclination is less than 42°. According to this, we can assume that *S.*

*angustirostris* gen. et sp. nov. had a significantly concave hard palate from its anterior part at least to P4–M1 as follows from the extremely sharp angle of P4 inclination (Fig. 4A<sub>1</sub>: a), and the “pectiniform” base of the antemolars. A similar angle, 44.5°, is exhibited in P4 of *Sorex caecutiens* Laxmann, 1785, while other species demonstrate angle values between 53° and 82°, leading to the following question. If the hard palate is concave, is the muzzle narrow? For determination of muzzle width, we took the distance between the left and right P4 (P4s/d), and the mandibular “short length” (MSL). Linear regression analysis identified the relationship between P4s/d and MSL for 9 soricine (SOM 6: fig. 2A) and 18 crocidurine (SOM 6: fig. 2B) species. The correlation in soricines was described as  $P4s/d = (0.266 \times MSL) - 0.435$ , with a high coefficient of correlation (0.908). In crocidurines  $P4s/d = (0.149 \times MSL) + 0.199$ , with a coefficient of 0.780. Using known MSL values of the Shargain shrew results in a calculated width between left and right P4 of 0.937–1.035 mm or 0.990–1.045 mm with the soricine and crocidurine datasets, respectively. Both intervals are similar, though the second one is narrower. Among small-sized soricine shrews, MSL values overlap with part of the *S. caecutiens* sample, but they probably have a narrower distance between left and right P4. Among small white-toothed shrews, our new species overlaps with *Sylvisorex johnstoni* (Dobson, 1887). A second LRA was performed for determination of the skull size of *S. angustirostris* gen. et sp. nov., using the relationships between MSL and condylo-incisive length (CIL) for all 27 soricine and crocidurine species. The linear relationship is described as  $CIL = (2.298 \times MSL) + 4.085$ , with a coefficient of correlation of about 0.965. Thus, the CIL of the Shargain shrew probably ranged between 16.2–17.1 mm. These values are approximately similar to the CIL of *C. shantungensis* (16.5–17.9 mm).

Using the available drawings of the transverse dissection at the level of the P4 root of several soricine and crocidurine shrews, we describe the specific shape of the antero-buccal root of P4 for each group: a straight root in crocidurines and a curved root in soricines. We illustrate both variants: the straight one of *Suncus etruscus* (Savi, 1822) (Fig. 4F<sub>1</sub>), and the curved one of *Sorex araneus* Linnaeus, 1758 (Fig. 4E<sub>1</sub>). Other studied species, such as *S. caecutiens*, *S. minutus*, *Blarina brevicauda* (Say, 1823), *C. suaveolens* (Pallas, 1811), *C. juvenetae* Heim de Balsac, 1958, and *C. yaldeni* Lavrenchenko, Voyta, and Hutterer, 2016 confirm this observation. Differentiation among these types is probably based on geometry of the lateral part of the rostrum. The Shargain shrew demonstrates a crocidurine-like straight root and rostrum construction. According to this, we used rostrum dissections of *C. suaveolens*, *C. juvenetae*, *S. johnstoni*, and a drawing of the left maxilla fragment of the Shargain shrew (see Fig. 4A<sub>1</sub>) to attempt a reconstruction of the rostrum shape for the latter. We found the geometrical relationship between the height and width of the rostrum among Recent shrews, which is expressed by the formula  $h = w/x$ , where  $x = \text{constant}$ ; i.e., this relationship was stable

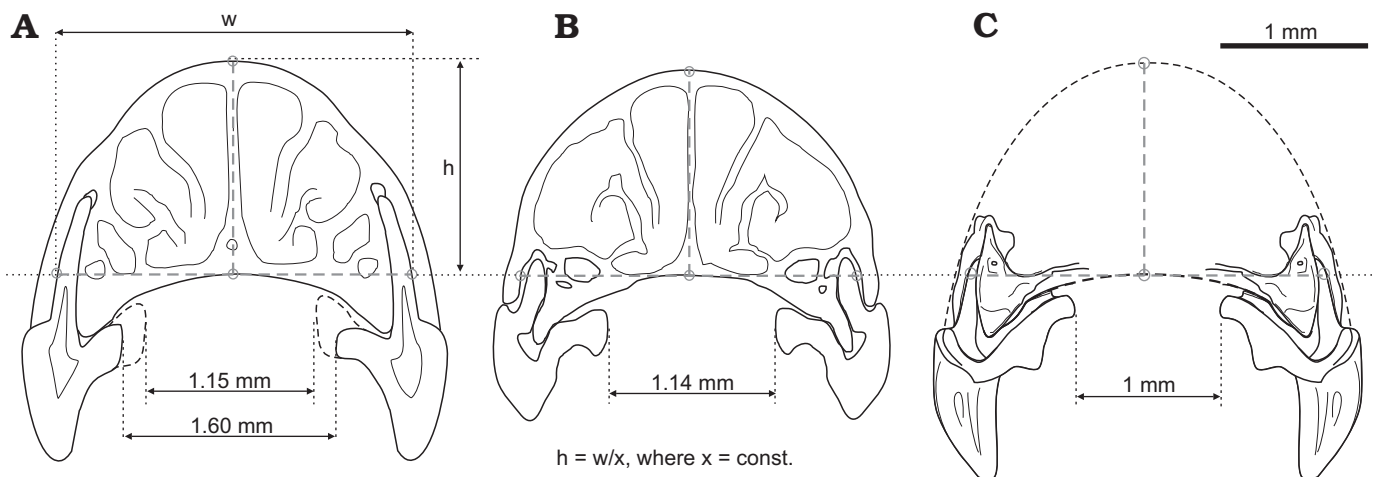


Fig. 9. Drawings of transverse section at the level of P4 antero-buccal root of two Recent crocidurine species (A, B), and reconstruction of the rostrum shape of *Shargainosorex angustirostris* gen. et sp. nov. (C). A. *Crocidura suaveolens* (Pallas, 1811) (ZISP 83089). B. *Sylvisorex johnstoni* (Dobson, 1887) (MNHN 1991-96). C. Combined drawings of the maxilla fragment. Correlation between  $h$  (height of rostrum) and  $w$  (width of rostrum between lateral sides of antero-buccal root of P4, via top point of the palatine arch) is approximately stable (at least for small-sized crocidurine shrews), and can be expressed by the formula  $h = w/x$ , where  $x = \text{const.}$

for several crocidurine species. Then, we combined drawings of the left maxilla fragments (left + its mirror view) of the fossil shrew, considering angles of tilting of the palatal part and P4 roots. Approximate width and height of the rostrum were determined with the above-mentioned formula. The final size of all reconstructed rostrum parts were calibrated by the measured distance between the left and right P4 (we took the mean value of distance between right and left P4: 1.01 mm). Figure 9C shows the approximate shape, size, and relative position of teeth of the Shargain shrew. Compared to *C. suaveolens* (CIL = 17.65 mm) and *S. johnstoni* (CIL = 14.86 mm), the relative width of the rostrum of *S. angustirostris* gen. et sp. nov. is a little narrower, and the P4 teeth are visibly close together. The narrow muzzle of the new species is likely correlated with the tilting of the lingual part of P4 and the relative large size of teeth, probably in relation to foraging adaptations.

## Conclusion

Crocidosoricinae is considered the ancestral group to other subfamilies of shrews, at least for Crocidurinae and Soricinae (Reumer 1987, 1994, 1998). Some Neogene soricide taxa have been demonstrated as evolutionary attempts at development along similar directions to both Recent groups, Soricinae and Crocidurinae. The Shargain shrew represents a dead-end evolutionary line of soricine-like shrews, as we can assume on the basis of several specific features (dental formula, tooth pigmentation, etc.) of the new species. According to Ziegler (1989) and Reumer (1994), the first Soricinae possibly appeared in the early Miocene, i.e., a morphological trend appears, leading to the subfamily Soricinae (Reumer 1987) or another extinct group with some soricine-like characters (Ziegler 1989), that was found

in *Carposorex* and *Crocidosorex*. Approximately at the same time, other non-soricine groups developed in parallel directions, but on a slightly different morphological basis. In comparison to the European taxa of *Miosorex* sensu lato (or any Neogene crocidosoricine taxa) the Asian Shargain shrew displays advanced morphological characters corresponding more closely to the evolutionary direction of Soricinae. This indicates a possible Central Asian origin of the process of “soricinization” of some shrew lines. According to common morphological characters between *S. angustirostris* gen. et sp. nov. and *M. pusilliformis*, and particular differences between each of them, we can cautiously assume a European origin for the new genus and a further spreading to the east with notable morphological changes. The appearance of reddish tooth pigment in the Shargain shrew was probably a consequence of the shifting to sorex-like metabolism (also including a slight reduction in body size) during the move from west to east, a possible, most parsimonious hypothesis. This “soricinization” trend of *Shargainosorex* gen. nov. simultaneously in *Sorex*, but true Soricinae from the middle Miocene remain unknown (this part of the fossil record is hidden), and the well-documented record of *Sorex* begins in the late Miocene of Europe (Rzebik-Kowalska 1998) and early Pliocene of Asia (Storch et al. 1998).

Another part of Shargain shrew morphology is similar to the evolutionary direction of crocidurines. The anterior-posterior “compression” of the upper and lower teeth as observed in *S. angustirostris* gen. et sp. nov. is not unique within Crocidurinae (e.g., *Diplomesodon pulchellum* (Lichtenstein, 1823) and *Suncus lixus* (Thomas, 1897)) and it is found in other Crocidosoricinae (e.g., *Turiasorex pierre-meini* Van Dam, Van den Hoek Ostende, and Reumer, 2011), but weakly expressed in typical Soricinae with the ancestral dental formula. The Shargain shrew bears five upper and two lower antemolars, similar to *Sorex*, but notable croc-

idurine-like tooth row compression, which is expressed in the disto-mesial compression of the upper antemolar crowns (alveoli), slight compression of upper molariform teeth (P4–M2), and buccal shifting of the a1 root as result of the lower antemolar row compression. The Shargain shrew is likely to have had a comparably narrow and long muzzle with large teeth as in *Sorex*, but the composition (geometry) of the lateral side of the rostrum and the type of P4 roots are as in *Crocidura* or *Suncus* sensu lato, i.e., a long and narrow muzzle (similar to *Sorex*), but highly domed (similar to *Crocidura*). Thus, *Shargainosorex* gen. et sp. nov. belongs to the subfamily Crocidosoricinae because it has clear important intermediate features of the two modern subfamilies. The new taxon undoubtedly is a dead-end evolutionary form illustrating an early attempt of “soricine evolution”. We are still not ready to answer the question: “When and where did the soricine-like crocidosoricine shrews lose the crocidurine features, and became real soricines?”, considering the clear temporal hiatus between the middle Miocene locality of Sharga 2 and the late Miocene deposits with true Soricinae members.

## Acknowledgements

Authors are grateful to Robert Emmanuel (University Lyon 1, France) who conducted an investigation of the transfer of some material from Vieux-Collonges and La Grive-Saint-Alban by Pierre Mein (Claude Bernard University Lyon 1, France) to colleagues from ZISP; to Alexei Miroljubov (ZISP) for technical support of SEM-images. We wish to thank Mikhail P. Zhurbenko, Anna A.Kijashko, and Evgenii S. Popov (all Botanic Institute of Russian Academy of Sciences, St. Petersburg, Russia) for organizing the tooth pigment investigations with the histological equipment of the Center for Collective Use of Scientific Equipment. We express our thanks to Christiane Denys, Violaine Nicolas, and François Jacquet (all National Museum of Natural History of Paris, France), and Leonid A. Lavrenchenko (A.N. Severtsov Institute of Ecology and Evolution, Moscow, Russia) for providing access to African specimens of Crocidurinae. Personal thanks to Dmitry Nagel (University of Dresden, Germany) for improving some of our German–English translations. Special thanks to Lars van den Hoek Ostende (Naturalis Biodiversity Centre, Leiden, The Netherlands), Jelle Reumer (Utrecht University, The Netherlands), and Mark Furió (Institut Català de Paleontologia, Cerdanyola del Vallès, Spain), who reviewed our manuscript and contributed to its improvement. This study was fulfilled within the framework of the Federal themes of the Theriology Laboratory of ZIN RAS AAAA-A17-117022810195-3 “Phylogeny, morphology and systematics of placental mammals”; it was supported by the Federal Agency for Scientific Organizations program for the support to bioresource collections; and it was partly financially supported by the Russian Foundation for Basic Research (project 16-04-00294 A).

## References

Archibald, J.D. 2003. Timing and biogeography of the eutherian radiation: fossils and molecules compared. *Molecular Phylogenetics and Evolution* 28: 350–359.

Asher, R. 2005. A morphological basis for assessing the phylogeny of the “Tenrecoidea” (Mammalia, Lipotyphla). *Cladistics* 15: 231–252.

Bendukidze, O.G., de Bruijn, H., and Van den Hoek Ostende, L.W. 2009. A revision of Late Oligocene associations of small mammals from the Aral Formation (Kazakhstan) in the National Museum of Georgia, Tbilissi. *Palaeodiversity* 2: 343–377.

Dannelid, E. 1998. Dental adaptations in shrew. In: J.M. Wójcik and M. Wolsan (eds.), *Evolution of Shrews*, 157–174. Mammal Research Institute Polish Academy of Sciences, Białowieża.

Daxner-Höck, G., Badamgarav, D., Barsbold, R., Bayarmaa, B., Erbajeva, M., Göhlich, U.B., Harzhauser, M., Höck, E., Höck, V., Ichinnorov, N., Khand, Y., López-Guerrero, P., Maridet, O., Neubauer, T., Oliver, A., Piller, W., Tsogtbaatar, K., and Ziegler, R. 2017. Oligocene stratigraphy across the Eocene and Miocene boundaries in the Valley of Lakes (Mongolia). *Palaeobiodiversity and Palaeoenvironments* 97: 111–218.

Depéret, C. 1892. La faune des mammifères de la Grive-Saint-Alban (Isère). *Archives du Muséum d’Histoire Naturelle de Lyon* 5: 1–93.

Doben-Florin, U. 1964. Die Spitzmäuse aus dem Altburdigalium von Wintershof-West bei Eichstätt in Bayern. *Abhandlungen der Bayerischen Akademie der Wissenschaften, mathematisch-naturwissenschaftliche Klasse (Neue Folge)* 117: 1–82.

Doukas, C. and Van den Hoek Ostende, L.W. 2006. Insectivores (Erinaceomorpha, Soricomorpha; Mammalia) from Karydia and Komotini (Thrace, Greece; MN 4/5). *Beiträge zur Paläontologie* 30: 109–131.

Dubey, S., Salamin, N., Ohdachi, S.D., Barrière, P., and Vogel, P. 2007. Molecular phylogenetics of shrews (Mammalia: Soricidae) reveal timing of transcontinental colonization. *Molecular Phylogenetics and Evolution* 44: 126–137.

Dumont, M., Tütken, T., Kostka, A., Duarte, M.J., and Borodin, S. 2014. Structural and functional characterization of enamel pigmentation in shrew. *Journal of Structural Biology* 186: 38–48.

Engesser, B. 2009. The Insectivores (Mammalia) from Sansan (Middle Miocene south-western France). *Schweizerische Paläontologische Abhandlungen* 128: 1–91.

Engesser, B. and Storch, G. 2008. Latest Oligocene Didelphimorpha, Lipotyphla, Rodentia and Lagomorpha (Mammalia) from Oberleichtersbach, Rhön Mountains, Germany. *Courier Forschungsinstitut Senckenberg* 260: 185–251.

Furió, M. and Pons-Monjo, G. 2013. The use of the species concept in paleontology. Comment on “*Nesiotites rafelinensis* sp. nov., the earliest shrew (Mammalia, Soricidae) from the Balearic Islands, Spain” by Rofes et al. 2012. *Palaeontologia Electronica* 16: 16.2.16A.

Furió, M., Santos-Cubedo, A., Minwer-Barakat, R. and Agusti, J. 2007. Evolutionary history of the african soricid *Myosorex* (Insectivora, Mammalia) out of Africa. *Journal of Vertebrate Paleontology* 27: 1018–1032.

Hammer, Ø. 2002. *Morphometrics—Brief Notes*. 49 pp. Paläontologisches Institut und Museum, Zürich. Available from: <http://folk.uio.no/ohammer/past/morphometry.pdf> (accessed 17 June 2015).

Hammer, Ø., Harper, D.A.T., and Ryan, P.D. 2001. PAST: Paleontological Statistics software package for and data analysis. *Palaeontologia Electronica* 4: 1–9.

Hammer, Ø., Harper, D.A.T., and Ryan, P.D. 2008. *PAST: Paleontological Statistics, ver. 1.87*. 88 pp. Available from: [http://www.academia.edu/2683729/PAST\\_Palaeontological\\_Statistics\\_ver\\_1.87](http://www.academia.edu/2683729/PAST_Palaeontological_Statistics_ver_1.87)

Hooker, J. 2017. Occlusal and morphogenetic field evolution in the dentition of European Nyctitheriidae (Euarchonta, Mammalia). *Historical Biology* 30: 42–52.

Hugueney, M. and Maridet, O. 2011. Early Miocene Soricids (Insectivora, Mammalia) from Limagne (Central France): new systematic comparisons, updated biostratigraphic data and evolutionary implications. *Geobios* 44: 225–236.

Hugueney, M., Mein, P., and Maridet, O. 2012. Revision and new data on the Early and Middle Miocene soricids (Soricomorpha, Mammalia) from central and south-eastern France. *Swiss Journal of Palaeontology* 131: 23–49.

Hutterer, R. 1993. Order Insectivora. In: D.E. Wilson and D.A. Reeder (eds.), *Mammal Species of the World: A Taxonomic And Geographic Reference*. 2nd. edition, 69–130. Smithsonian Institution Press, Washington.

Hutterer, R. 2005. Order Soricomorpha. In: D.E. Wilson and D.A. Reeder (eds.), *Mammal Species of the World: A Taxonomic And Geographic*

- ic Reference. 3rd edition. Vol. 1, 220–311. Johns Hopkins University Press, Baltimore.
- Klietmann, J., Nagel, D., Rummel, M., and Van den Hoek Ostende, L.W. 2013. Tiny teeth of consequence: vestigial antemolars provide key to Early Miocene soricid taxonomy (Eulipotyphla: Soricidae). *Comptes Rendus Palevol* 12: 257–267.
- Klietmann, J., Nagel, D., Rummel, M., and Van den Hoek Ostende, L.W. 2014. *Heterosorex* and Soricidae (Eulipotyphla, Mammalia) of the fissure Petersbuch 28; micro-evolution as indicator of temporal mixing? *Comptes Rendus Palevol* 13: 157–181.
- Koenigswald, W. von 2016. Specialized wear facets and late ontogeny in mammalian dentitions. *Historical Biology* 30: 7–29.
- Lartet, E. 1851. *Notice sur la colline de Sansan*. 47 pp. J.A. Portes, Imprimeur de la Préfecture et Libraire, Auch.
- Lavrenchenko, L.A., Voyta, L.L. and Hutterer, R. 2016. Diversity of shrews in Ethiopia, with the description of two new species of *Crociodura* (Mammalia: Lipotyphla: Soricidae). *Zootaxa* 4196: 38–60.
- Li, C., Lin, Y., Gu, Y., Hou, L., Wu, W. and Qiu, Z. 1983. The Aragonian vertebrate fauna of Xiacaowan, Jiangsu. 1. A brief introduction to the fossil localities and preliminary report on the new material. *Vertebrata Palasiatica* 21: 313–327.
- Lopatin, A.V. 2004. New Early Miocene shrews (Soricidae, Mammalia) from Kazakhstan. *Paleontological Journal* 38: 211–219.
- Lopatin, A.V. 2006. Early Paleogene insectivore mammals of Asia and establishment of the major group of Insectivora. *Paleontological Journal* 40 (Supplement 3): 205–405.
- Lopatin, A.V. and Zazhigin, V.S. 2003. New Brachyericinae (Erinaceidae, Insectivora, Mammalia) from the Oligocene and Miocene of Asia. *Paleontological Journal* 37: 62–75.
- Maddalena, T. and Bronner, N. 1992. Biological systematics of the endemic African genus *Myosorex* Gray, 1838 (Mammalia: Soricidae). *Israel Journal of Zoology* 38: 245–252.
- McKenna, M.C. and Bell, S.K. 1997. *Classification of Mammals Above the Species Level*. 631 pp. Columbia University Press, New York.
- Miller, R.L. and Kahn, J.S. 1962. *Statistical Analysis in the Geological Sciences*. 483 pp. John Wiley & Sons, New York.
- Öztuna, D., Elhan, A.H., and Tüccar, E. 2006. Investigation of four different normality tests in terms of type 1 error rate and power under different distributions. *Turkish Journal of Medical Sciences* 36: 171–176.
- Qiu, Z. 1988. Neogene micromammals of China. In: P. Whyte, J.S. Aigner, N.G. Jablonski, G. Taylor, D. Walker, and P.X. Wang (eds.), *Paleoenvironment of East Asia from the mid-Tertiary (Second International Conference on the Paleoenvironment of East Asia)*, 834–848. Centre of Asian Studies, University of Hong Kong, Hong Kong.
- Qiu, Z. 1996. *Middle Miocene Micromammalian Fauna from Tunggur, Nei Mongol*. 216 pp. Science Press Beijing, Beijing.
- Quérouil, S., Hutterer, R., Barrière, P., Colyn, M., Peterhans, J.C.K., and Verheyen, E. 2001. Phylogeny and evolution of African shrews (Mammalia: Soricidae) inferred from 16S rRNA sequences. *Molecular Phylogenetics and Evolution* 20: 185–195.
- Repenning, C.A. 1967. Subfamilies and genera of the Soricidae. Classification, historical zoogeography and temporal correlation of the shrews. *United States Survey Professional Paper* 565: 1–74.
- Reumer, J.W.F. 1984. Ruscian and Early Pleistocene Soricidae (Insectivora, Mammalia) from Tegelen (The Netherlands) and Hungary. *Scripta Geologica* 73: 1–173.
- Reumer, J.W.F. 1987. Redefinition of the Soricidae and the Heterosoricidae (Insectivora, Mammalia) with the description of the Crocidosoricinae, a new subfamily of Soricidae. *Revue de Paléobiologie* 6: 189–192.
- Reumer, J.W.F. 1994. Phylogeny and distribution of the Crocidosoricinae (Mammalia: Soricidae). In: J.F. Merrit, G.L. Kirkland, and R.K. Rose (eds.), *Advances in the Biology of Shrews. Special Publication 18*, 345–356. Carnegie Museum of Natural History, Pittsburgh.
- Reumer, J.W.F. 1998. A classification of fossil and recent shrews. In: J.M. Wójcik and M. Wolsan (eds.), *Evolution of Shrews*, 5–22. Mammal Research Institute Polish Academy of Sciences, Białowieża.
- Rofes, J., Bover, P., Cuenca-Bescós, G., and Alcover, J.A. 2012. *Nesiotites rafelinensis* sp. nov., the earliest shrew (Mammalia, Soricidae) from the Balearic Islands, Spain. *Palaentologia Electronica* 8A 15: 1–12.
- Rohlf, F.G. and Slice, D.E. 1990. Extension of the Procrustes method for the optimal superimposition of landmarks. *Systematic Zoology* 39: 40–59.
- Rzebik-Kowalska, B. 1993. Insectivora (Mammalia) from the Miocene of Belchatów in Poland. I. Metacodontidae: *Plesiosorex* Pomel, 1854. *Acta zoologica cracoviensis* 36: 267–274.
- Rzebik-Kowalska, B. 1998. Fossil history of shrews in Europe. In: J.M. Wójcik and M. Wolsan (eds.), *Evolution of Shrews*, 23–92. Mammal Research Institute Polish Academy of Sciences, Białowieża.
- Sarà, M., Valvo, M.L., and Zanca, L. 1990. Insular variation in central Mediterranean *Crociodura* Wagler, 1832 (Mammalia, Soricidae). *Bollettino di Zoologia Italiana* 57: 283–293.
- Shapiro, S.S. and Wilk, M.B. 1965. An analysis of variance test for normality. *Biometrika* 52: 591–611.
- Smith, T. and Codrea, V. 2015. Red iron-pigmented tooth enamel in a Multituberculata Mammal from the Late Cretaceous Transylvanian “Hateg Island”. *PLOS ONE* e0132550 10: 1–16.
- Storch, G., Qiu, Z., and Zazhigin, V. 1998. Fossil history of shrews in Asia. In: J.M. Wójcik and M. Wolsan (eds.), *Evolution of Shrews*, 93–120. Mammal Research Institute Polish Academy of Sciences, Białowieża.
- Strait, S.G. and Smith, S.C. 2006. Elemental analysis of soricine enamel: pigmentation variation and distribution in molars of *Blarina brevicauda*. *Journal of Mammalogy* 87: 700–705.
- Van Dam, J.A., Van den Hoek Ostende, L.W., and Reumer, J.W.F. 2011. A new short-snouted shrew from the Miocene of Spain. *Geobios* 44: 299–307.
- Van den Hoek Ostende, L.W. 2001. Insectivore Faunas from the Lower Miocene of Anatolia. Part 6: Crocidosoricinae. *Scripta Geologica* 122: 47–81.
- Van den Hoek Ostende, L.W. 2003. Insectivores (Erinaceomorpha, Soricomorpha, Mammalia) from the Ramblian of the daroca-Calamocha area. In: N. López-Martínez, P. Peláez-Campomanes, and M. Hernández Fernández (eds.), *En torno a fósiles de mamíferos: datación, evolución y paleoambiente. I. Coloquios de Paleontología, Volumen extraordinario*, 281–310. Madrid.
- Viret, J. and Zapfe, H. 1951. Sur quelques soricidés miocènes. *Eclogae Geologicae Helveticae* 44: 411–426.
- Wible, J.R. 2008. On the cranial osteology of the hispaniolan solenodon, *Solenodon paradoxus* Brandt, 1833 (Mammalia, Lipotyphla, Solenodontidae). *Annals of Carnegie Museum* 77: 321–402.
- Zaitsev, M.V. and Rzebik-Kowalska, B. 2003. Variation and taxonomic value of some mandibular characters in red-toothed shrews of the genus *Sorex* L. (Insectivora, Soricidae). *Russian Journal of Theriology* 2: 97–104.
- Zaitsev, M.V., Voyta, L.L., and Sheftel, B.I. 2014. *The Mammals of Russia and adjacent territories: Lipotyphlans. Vol. 178* [in Russian]. 391 pp. Izdatel'stvo Nauka, St. Petersburg.
- Zazhigin, V.S. and Lopatin, A.V. 2000. The History of the Dipodoidea (Rodentia, Mammalia) in the Miocene of Asia: 1. *Heterosminthus* (Lophocricetinae). *Paleontological Journal* 34: 319–332.
- Ziegler, R. 1989. Heterosoricidae and Soricidae (Insectivora, Mammalia) aus dem Oberoligozän und Untermiozän Süddeutschlands. *Stuttgarter Beiträge zur Naturkunde* 154: 1–73.
- Ziegler, R. 1990. Didelphidae, Erinaceidae, Metacodontidae und Dimylidae (Mammalia) aus dem Oberoligozän und Untermiozän Süddeutschlands. *Stuttgarter Beiträge zur Naturkunde. Serie B (Geologie und Paläontologie)* 158: 1–99.
- Ziegler, R. 2005. Erinaceidae and Dimylidae (Lipotyphla) from the Upper Middle Miocene of South Germany. *Senckenbergiana lethaea* 85: 131–152.
- Ziegler, R., Dahlmann, T. and Storch, G. 2007. Oligocene–Miocene vertebrates from the Valley of Lakes (Central Mongolia): morphology, phylogenetic and stratigraphic implications. 4. Marsupialia, Erinaceomorpha and Soricomorpha (Mammalia). *Annalen des Naturhistorischen Museums in Wien* 108A: 53–164.